RANDOM SIGNAL ULTRASONIC BLOOD FLOW DETECTION

Thesis for the Degree of M. S.

MICHIGAN STATE UNIVERSITY

FRANK SAGGIO III

1973

MICHIGAN STATE UNIVERSITY LIBRARIES
3 1293 00383 8731

LIBRARY
Michigan State
University

MICHIGAN STATE UNIVERS
LIBRARY
[redacted]

[redacted]

MICHIGAN STATE UNIVERSITY
LIBRARY

[redacted]

ABSTRACT

RANDOM SIGNAL ULTRASONIC BLOOD FLOW DETECTION

By

Frank Saggio III

Although conventional pulsed or continuous ultrasonic Doppler systems are used for transcutaneous blood flow detection with considerable success, it is found that these systems are severely limited by signal-to-noise ratio problems; particularly when used on deep-lying vessels such as the superior vena cava, or on patients with emphysema where good signals are difficult to obtain.[1] In addition, because of the periodic nature of these conventional signals, ambiguities in target range or blood velocity measurement may occur even when examining periphereal vessels.

The objective of this thesis is to propose and examine concepts which will improve the performance of ultrasonic blood flow sensing systems.

A random signal ultrasonic system is described which uses a digital correlator and several bandpass filters to extract the target range and velocity information. A model of the random signal system is presented and analyzed to give the basic equations describing the system. Longitudinal

range and velocity resolution are shown to be independently controllable. The performance capabilities of the random signal system are compared to those of a conventional pulsed system.

An experimental random signal ultrasonic system used to make in-vitro Doppler frequency measurements is described. The transmitted signal consists of 10 μsec pulses of random noise with a center frequency of 4.59 MHz and a bandwidth of 4 MHz. Results are presented which indicate that the experimental system is capable of measuring the Doppler difference frequency within an error range of $\pm$ 1%.

The theory and operation of a dual element broadband transducer designed for ultrasonic blood flow detection is presented. The novel transducer is compared with a single element transducer in terms of lateral range resolution. The experimental results indicate a marked increase in lateral resolution with the dual element transducer.

Two methods for determining the angles associated with Doppler blood flow measurement are described.

---

[1] K. L. Gould, D. J. Mozersky, D. E. Hokanson, D. W. Baker, J. W. Kennedy, D. S. Sumner, and D. E. Strandness, Jr., "A noninvasive technique for determining potency of saphenous vein coronary bypass grafts," Circulation, Volume XLVI, pp. 595-600, September 1972.

RANDOM SIGNAL ULTRASONIC
BLOOD FLOW DETECTION

By

Frank Saggio III

A THESIS

Submitted to
Michigan State University
in partial fulfillment of the requirements
for the degree of

MASTER OF SCIENCE

Department of Electrical Engineering
and Systems Science

1973

G84627

To all of my families

ACKNOWLEDGMENTS

I thank Dr. C. P. Jethwa for his assistance and guidance throughout the duration of this project. The labor involved in writing this thesis was considerably lightened by his help in preparing a detailed outline.

I wish to thank Philip A. Priest for exhibiting an occasional counterexample of excellence. He is responsible for many of the drawings found in this thesis.

Appreciation is extended to the General Motors Corporation for providing the financial support which has made my graduate study and this thesis possible.

TABLE OF CONTENTS

Chapter Page

LIST OF TABLES

LIST OF FIGURES

CHAPTER I

INTRODUCTION

1.1 The Importance of Blood Flow Studies

Volume blood flow measurement is important in determining the amount of oxygen being delivered to various regions of the body. Also, knowledge of the acceleration of the blood flow in the ascending aorta or other large vessels may be useful in assessing the performance of the heart [5]. This volume blood flow information is normally obtained by measuring the mean blood flow velocity and the vessel's cross-sectional area at a particular site.

The determination of a velocity profile in arteries may be useful in identifying arteriosclerosis by distinguishing a laminar flow from a turbulent flow. This method may also provide a basis for the early identification of turbulent areas in atherosclerotic arteries.

Blood velocity profile, volume flow and average flow velocity measurements also provide information about the blood viscosity, which is known to be an important factor in the etiology of ischemic diseases [24].

From the above discussion it is clear that quantitative blood flow information is often essential before a

particular disease can be properly diagnosed. At present, cardiac catherization and angiography techniques are used to access many of the aforementioned physiological parameters. However, these invasive techniques are limited in their routine use in postoperative studies because of the potential mortality associated with their repeated application [6,26]. For this reason there is a strong interest in the development of a noninvasive ultrasonic method for measuring these parameters. This thesis describes the feasibility of such an ultrasonic system which can measure with a high degree of spatial resolution, many of the above physiological quantities.

The following section summarizes the conventional ultrasonic methods and devices for determining the blood flow velocity.

1.2 Review of the Existing Blood Flow Meters

Several different techniques, from plethysmography to nuclear magnetic resonance, have been used for detection and measurement of blood flow. The major difficulty with these methods is the lack of specificity required to sense flow at a particular site [5]. Ultrasonic techniques do not suffer from such handicaps and hence are ideally suited for medical research, diagnosis and treatment.

Franklin [30], Wells [22], and Baker [5] have published excellent surveys of various ultrasonic blood flow meters. The existing ultrasonic devices can be classified into one of two broad categories: the transmission type or the reflection type. Continuous or pulsed ultrasonic waves can be used with either type flowmeter.

1.2.1 Transmission-type Ultrasonic Flow Meters

These flow meters are based on the principal that a sound beam, passed diagonally through a blood vessel, would exhibit a difference in the time required to traverse the vessel alternately in the upstream and downstream directions. The average blood velocity v of the medium can be determined by using the following relationship:

$$v = \frac{\Delta t \cdot c^2}{2d \cdot \cos\theta} \tag{1}$$

where Δt is the measured difference between the upstream and downstream transit times, c is the velocity of ultrasound relative to the propagating medium, d is the distance between two transducers placed diagonally on either side of the vessel, and θ is the angle between the axis of ultrasound propagation and the flow axis. Figure 1 illustrates a typical transducer arrangement.

Many transmission type flow meters have been designed. Kalmus [31] developed an instrument to measure fluid velocity by noting that a continuous ultrasonic wave transmitted alternately upstream and downstream would produce a phase difference proportional to the average velocity of the medium through which the sound passes. Haugen et al. [32] and Baldes et al. [33] used modified versions of the instrument developed by Kalmus.

Franklin et al. [34,35] experimented with a pulsed ultrasonic flow meter. The upstream and downstream transit times for 3 MHz ultrasonic pulses were compared by considering the amplitudes of corresponding ramps generated by a time-to-voltage analog converter.

Farall [36] improved the earlier system of Baldes [33] by using two transmitter and receiver pairs. The reference signal from each transmitter was compared with its respective received signal by a phasemeter. The difference between the outputs of the two phasemeters was proportional to the flow velocity.

Zarnstroff et al. [37] reported an instrument in which a continuous 1 MHz signal was transmitted alternately upstream and downstream. The received signal was heterodyned to 10 KHz. Differences in the upstream and downstream phase of the 10 KHz signal were proportional to the flow velocity. Noble et al. [38] reported a phase shift technique which eliminated the need for switching the sound path upstream and downstream, and hence improved the high frequency response of the system.

The performance of transmission type flowmeters is very unsatisfactory at velocities below 10 cm/sec. But the

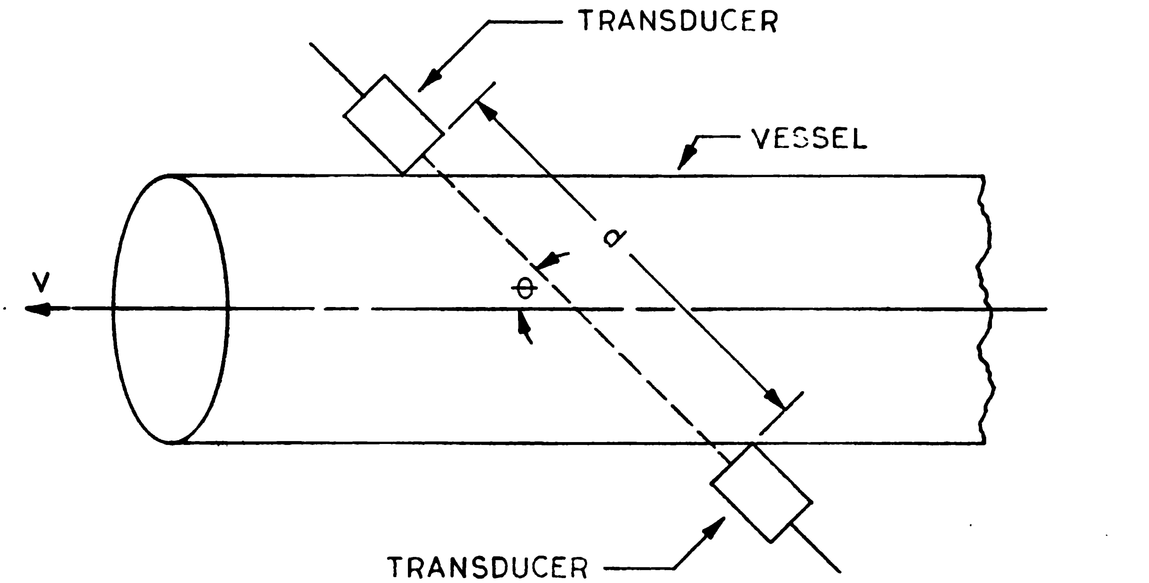

Figure 1.--Arrangement of Transducers for Measurement of Flow Velocity by Transit Time Difference in Up and Down Stream Paths.

main disadvantage associated with these flow detectors is that surgery must be performed to fasten the transducers and holder directly to the blood vessel. Consequently as reported by Wetterer [39], the transmission type ultrasonic flow meter is no better than the electromagnetic flow detector.

1.2.2 Reflection-type Ultrasonic Flow Meters

These flowmeters are based on the principal of the Doppler effect. When ultrasound is transmitted into the blood stream, a portion of the signal is scattered by the moving blood particles. The frequency of the back-scattered sound is Doppler shifted. The relationship between the average Doppler difference frequency f_d and the average blood flow velocity v is given by the following equation [22,40]

$$v = \frac{c \cdot f_d}{f_o \cdot (\cos\alpha - \cos\beta)} \qquad (2)$$

where c is the velocity of ultrasound in blood, f_o is the transmitted ultrasonic frequency, α is the angle between the transmitted ultrasonic beam and the velocity vector, and β is the angle between the reflected ultrasonic beam and blood velocity vector. Figure 2 illustrates a typical transducer arrangement.

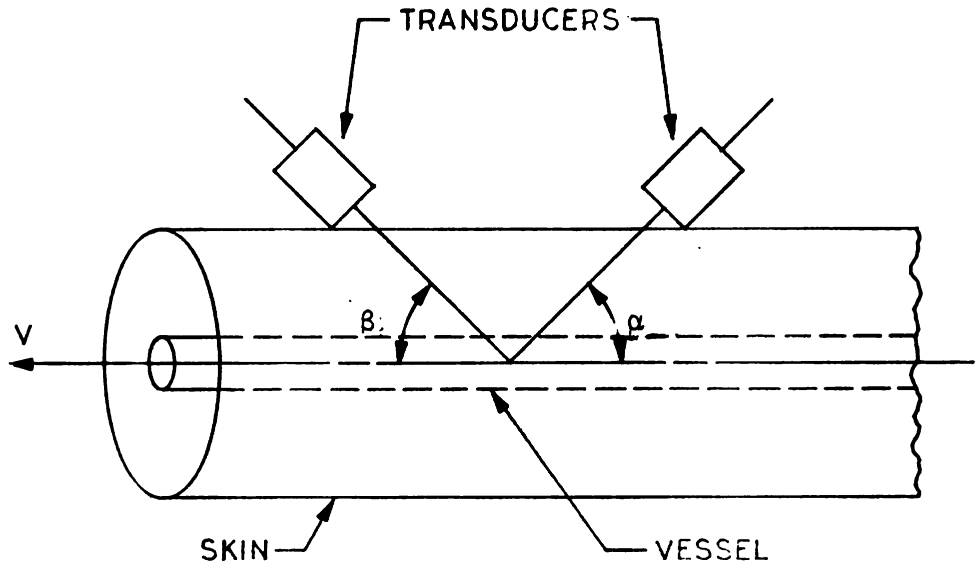

Figure 2.--Arrangement of Transducers for Measurement of Flow Velocity by Reflection Methods.

Reflection-type devices may operate in the continuous wave mode or the more sophisticated pulsed Doppler mode. Satomura [42] was first to demonstrate continuous wave Doppler motion detection in 1956. Franklin _et al_. [43] used this technique for blood velocity detection in animals. Baker [44] developed a practical instrument for the transcutaneous detection of blood flow in humans.

The early continuous wave flow meters were not capable of detecting the direction of the blood velocity vector with respect to the transducer. In 1966 McLeod [45,46] used a version of quadrature phase detection common to single sideband radio techniques to demonstrate the first successful direction sensing Doppler device. Yoshitoshi _et al_. [47] described another method of direction sensing.

Continuous wave blood flow detectors have found wide application in medical research. However, one of the greatest shortcomings of the continuous wave device is its inability to obtain a measurement of range. The continuous wave technique is inherently sensitive to all movement along the length of the sound beam. This lack of range sensitivity prevents the measurements of vessel diameter and velocity profile.

In order to preserve the range information, Moving Target Indicator (MTI) or pulsed Doppler radar techniques have been employed. Barnes and Thurstone [49] have developed an MTI ultrasonic system which uses a delay line canceler to filter the clutter echoes and pass only the Doppler frequency shifted signals returned from moving targets. However, this system is limited by the additional complexity required to achieve special filter characteristics which maximize the output signal-to-noise ratio. The technique is also hampered by the need to maintain perfect delay line adjustments in spite of temperature changes. For these reasons the pulse-Doppler system is preferred to the MTI system.

In the pulse-Doppler system a burst of ultrasound is transmitted. The distance to the dynamic target and its velocity with respect to the ultrasonic beam are determined by range-gating the return echoes. These received echoes are both phase and amplitude modulated by the moving target. The Doppler frequency or velocity information can be obtained by non-coherent or coherent detection.

The non-coherent pulsed-Doppler system makes use of the amplitude fluctuations in the echo signal to recognize the Doppler component produced by a moving target. Range-gating is used to select an echo for detection from a pre-determined depth. A linear or logarithmic receiver is necessary to preserve the amplitude components. The Doppler difference frequency is detected from the range-gated sample by a square law diode detector. The primary difficulty with the non-coherent technique is the erratic fluctuation in the detected Doppler signal due to the presence of noise clutter components. No blood flow detectors based on this principal are reported in the literature.

In a coherent pulsed-Doppler system, the range-gated echo is compared with a sample of the original transmitted signal in a phase detector to extract the Doppler components. A number of coherent systems have been built and used for measuring blood velocity, volume blood flow, and for mapping the lumen of the blood vessels [5,50-54].

Conventional pulsed-Doppler systems are generally inadequate for transcutaneous blood flow measurements in deep-lying vessels such as the ascending aorta, superior vena cava, or renal artery [6,23]. A significant improvement of the system's signal-to-noise ratio is required to increase the detection depth without exceeding the safe ultrasonic intensity level established for humans [27,28]. An increase in lateral resolution is also required to apply the pulsed-Doppler methods to very small vessels.

It is known that if n pulses each with the same signal-to-noise ratio were ideally integrated, the resultant signal-to-noise ratio would be exactly n times that of a single pulse [55]. However conventional pulsed-Doppler systems cannot use this method of enhancing signal-to-noise ratios without destroying the range information.

The range resolution capability of conventional pulse-echo systems is normally increased by narrowing the transmitted pulse. Two basic difficulties arise with this method. The first is generating and processing the transmitted and received signals. The second is maintaining sufficient average power in the transmitted signals. The usual requirement for a non-ambiguous range determination limits the maximum pulse repetition frequency. Thus, as the pulse width is narrowed, the amount of peak power required to maintain sufficient average power soon becomes unreasonable. Perhaps it may exceed the safe intensity level for tissues.

The solution to these inherent problems associated with conventional pulse-Doppler lies in the use of transmitted signals having a larger time-bandwidth product than a simple pulse [62]. The transmitted waveform may have a longer duration for the same range resolution capability, as in pulse compression or pseudo-random phase coded techniques. Or the signal may be transmitted at a higher repetition rate without range ambiguities, as in pseudo-noise sequences or signals using pulse-to-pulse frequency hopping.

Wagg and Gramiak [56,57] have developed a system utilizing the continuous transmission of a carrier which is phase modulated with a pseudo-random binary sequence. They have reported an enhancement in the signal processing gain over the conventional pulse-Doppler system. However, the improvement which is obtained with this technique is somewhat limited by the complexity of the equipment required to generate and process these signals. Also, because of the periodic nature of these signals, ambiguities in target range or velocity may still occur.

1.3 Preview of the Random Signal Ultrasonic System

A random signal pulse-Doppler system may provide the solution to the above problems. The use of transmitted signals derived from wideband Gaussian noise permits extremely large time-bandwidth products to be obtained and eliminates the difficulties with range and velocity ambiguities characteristic of periodic signals. Range and velocity resolution can be shown to be independently controllable. The signal-to-noise ratio may be enhanced many times by integrating the returns from successive pulses without destroying spatial resolution.

In Chapter II a generalized model of the random signal pulse-Doppler system is presented and analyzed to give the basic equations describing the operation of the system.

Chapter III describes the experimental system built and the results obtained for the Doppler resolution.

Chapter IV discusses the theory and operation of a novel transducer which improves the lateral resolution of the pulse-Doppler system.

In Chapter V methods for determining the angles associated with ultrasonic blood flow measurement are described and analyzed.

Chapter VI presents a summary of the results obtained and some recommendations for further experimental work.

CHAPTER II

THEORY AND GENERAL DESCRIPTION OF THE RANDOM SIGNAL ULTRASONIC SYSTEM

2.1 Introduction

The theory and effectiveness of the random signal microwave system are well documented [58-61]. In order to apply this technology to biomedical measurements it is necessary to change the transmitted signal from microwave electromagnetic radiation to wideband acoustical energy which is more suitable for propagation in living tissues. The concepts of resolution, accuracy, ambiguity, detection and clutter which are common in radar discussion, have their counterparts in the ultrasonic system with appropriate changes in the scale factors. A brief discussion of the theory of operation and a general description of the random signal ultrasonic system are presented in the following sections.

2.2 Basic Model of the Random Signal Ultrasonic System

The basic block diagram of the random signal system is shown in Figure 3. The transmitted signal $x(t)$ is assumed to be a sample function from a stationary zero mean

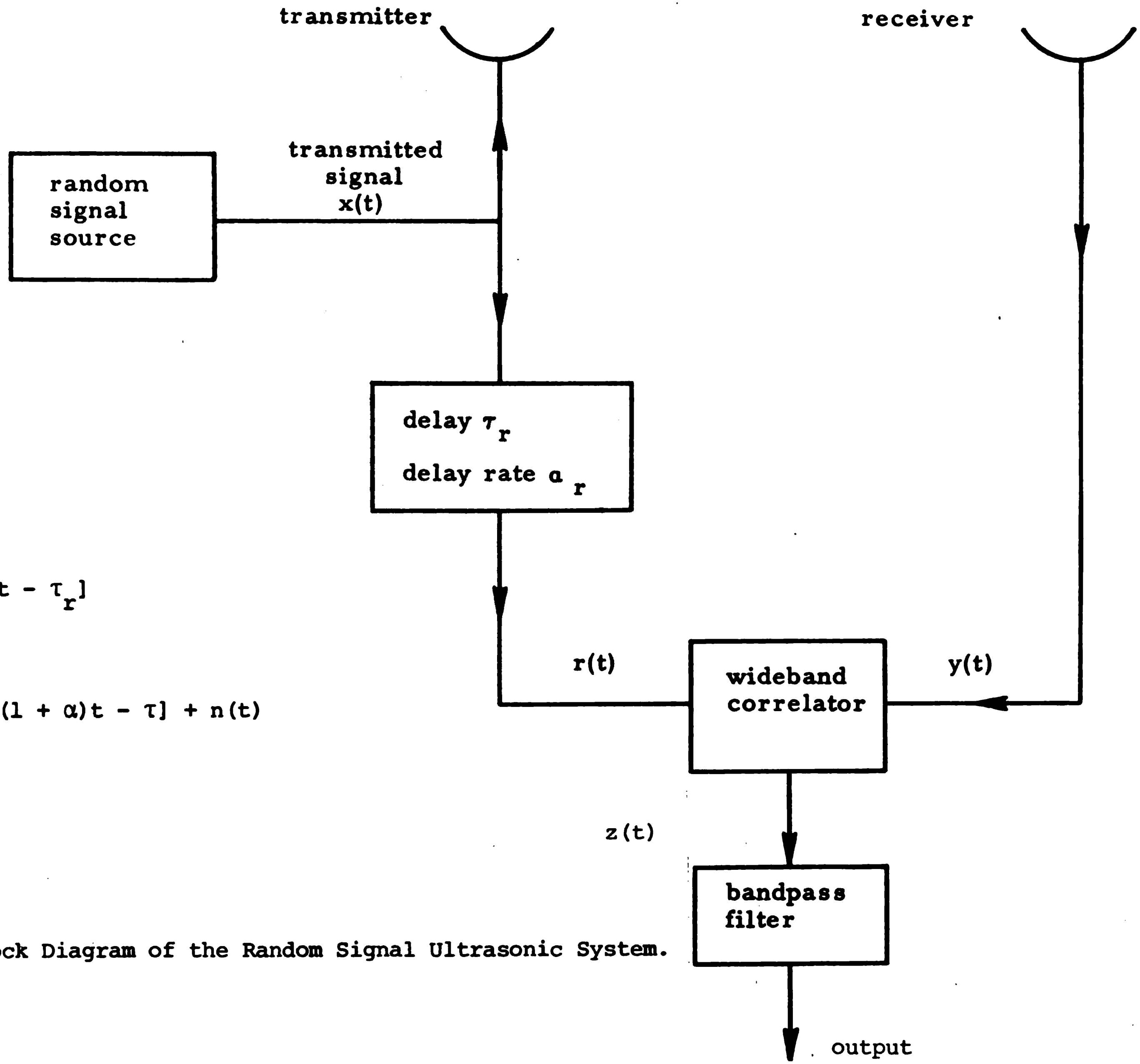

Reference signal

$$r(t) = x[(1 + \alpha_r)t - \tau_r]$$

Received signal

$$y(t) = a(\tau) \cdot x[(1 + \alpha)t - \tau] + n(t)$$

Figure 3.--Basic Block Diagram of the Random Signal Ultrasonic System.

random process generated by a random noise source. A portion of the transmitted signal is used to simulate the delay and Doppler shift of a fictitious target. This signal r(t) becomes the reference input to the correlator. The rest of the transmitted electrical signal is converted to acoustic energy by applying it to the input of a piezoelectric transducer which is used as a transmitter and is aimed at the living tissue. The reflected acoustic signal is converted back to an electrical signal by a piezoelectric receiving transducer. A single transducer is normally adequate for both transmission and reception of pulsed signals.

The reflected signal y(t) will be an amplitude scaled and delayed version of the transmitted signal plus it will contain a noise term. This signal provides the other input to the wideband correlator. The output of the correlator z(t) is the estimate of the cross-correlation function of y(t) and r(t).

By providing a bandpass filter after correlation the effects of the noise term are reduced. In addition, those portions of the cross-correlation function which do not represent targets of interest are eliminated. Thus the bandpass filter provides both the correlator smoothing time and the desired velocity resolution. This point will be discussed in detail later on.

Although the actual implementation of the cross-correlator is digital, it is simpler to discuss the theory in terms of an equivalent analog system. The digital processor achieves the same end results; the only basic difference is the requirement of longer processing time in the digital version. Unless otherwise stated, the analysis of Chapter II will assume the ultrasonic system is performing a continuous cross-correlation.

2.3 Theory of Operation

For ease in discussion let the transmitted signal $x(t)$ be a sample function from a stationary random process having a spectral density that is symmetrical about some center frequency f_c. Suppose at time $t = o$, there exists a single point target at range r, moving with a constant radial velocity v. Then the round trip time delay τ and the delay rate α associated with the signal returned from this target are given by

$$\tau = \frac{2r}{c} \tag{3}$$

$$\alpha = \frac{2v}{c-v} \simeq \frac{2v}{c} \tag{4}$$

where c is the propagation velocity of the acoustic signal in living tissues.

The returned signal $y(t)$, consisting of the reflected signal from the single point target and the system noise, can therefore be written as

$$y(t) = a(\tau) \cdot x[(1 + \alpha)t - \tau] + n(t) \tag{5}$$

where the attenuation coefficient $a(\tau)$ is real and between zero and one, and $n(t)$ is the system noise term. The noise term $n(t)$ is assumed to be zero mean and independent of $x(t)$.

This received signal $y(t)$ is cross-correlated with a reference signal $r(t)$ which has the following mathematical form

$$r(t) = x[(1 + \alpha_r)t - \tau_r] \tag{6}$$

with τ_r and α_r the delay time and delay rate respectively for the reference signal $r(t)$. These parameters (τ_r and α_r) can be adjusted at will and can be made to match a particular target reflecting point.

The correlator output $z(t)$ provides an estimate of the cross-correlation function. The expected value of $z(t)$, which is the desired correlator output, is given by

$$E\{z(t)\} = E\ \{[a(\tau)x[(1+\alpha)t-\tau] + n(t)] \cdot x[\ (1+\alpha_r)t-\tau_r)]\} \tag{7}$$

or, since $n(t)$ is assumed to be zero mean and independent of $x(t)$,

$$E\{z(t)\} = \overline{a(\tau)} \cdot R_x[(\alpha_r-\alpha)t-(\tau_r-\tau)] \tag{8}$$

where $R_x\ (\cdot)$ is the autocorrelation function of $x(t)$, and $\overline{a(\tau)}$ is the mean value of the attenuation coefficient.

Since $R_x(\cdot)$ is the autocorrelation function of a bandpass random process, it can be written in terms of a slowly varying envelope and cosine term

$$E[z(t)] = a\overline{(\tau)} \cdot R_c[(\alpha_r-\alpha)t-(\tau_r-\tau)]\cos\omega_c \cdot [(\alpha_r-\alpha)t-(\tau_r-\tau)] \tag{9}$$

where $R_c(\cdot)$ is the envelope of the correlation function and ω_c is the center frequency about which the spectral density of the transmitted signal x(t) is symmetrical.

The expected correlator output (equation 9) is depicted in Figure 4. The radian frequency of the output is

$$\omega = \omega_c \cdot (\alpha_r - \alpha) \tag{10}$$

and the time at which the peak occurs is

$$t_p = \frac{\tau_r - \tau}{\alpha_r - \alpha} \tag{11}$$

Figure 4 is a replica of the autocorrelation function of x(t) except that it has been stretched in time by a scale factor of $1/(\alpha_r - \alpha)$. Hence it will have a center frequency of $(\alpha_r - \alpha) \cdot f_c$ and this frequency will typically be in the audio range. Therefore a suitable filter at the output of the correlator will accept or reject this component as desired (See Figure 3). Since α depends upon the velocity of the reflecting point, points with different velocities will produce outputs with different center frequencies. Thus

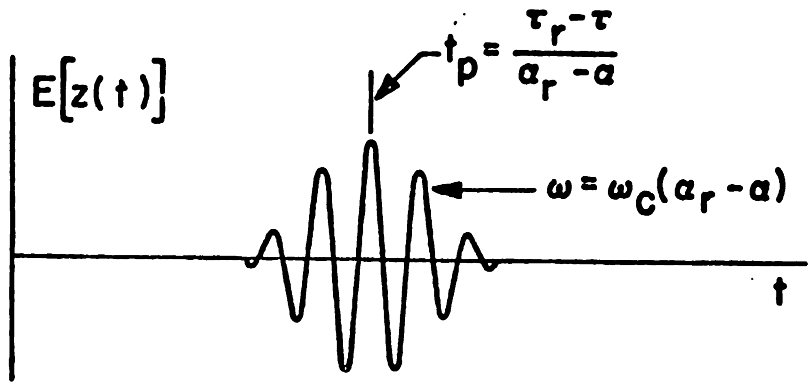

Figure 4.--Expected Correlator Output.

the ability of the ultrasonic system to resolve targets at the same range but having different velocities depends primarily upon the bandwidth of the filter at the output of the correlator. If the bandwidth of this filter is W, then by combining equations 4 and 10 it is easy to show that the velocity resolution of the system will be on the order of

$$\Delta v = \frac{c \cdot W}{2f_c} \tag{12}$$

where c is the propagation velocity of the acoustic wave in living tissues (approximately 1.48×10^5 cm/sec). For a bandlimited transmitted signal with center frequency f_c = 5 MHz and the bandwidth of the filter following correlation equal to W = 10Hz, the velocity resolution Δv is about .15 cm/sec.

When reflecting points are separated in range their responses in the correlator output will occur at different times. Hence, the ability to resolve targets having the same velocity but different target ranges depends upon the time separation of the responses (which have also been increased by the factor $1/(\alpha_r - \alpha)$) compared to the expanded width of the autocorrelation function. Again it is easy to show that if the transmitted signal has a bandwidth B, which determines the width of the correlation function, the range resolution ΔR is on the order of

$$\Delta R = \frac{c}{2B} \tag{13}$$

where c is the propagation velocity of the acoustic wave (roughly 1.48×10^5 cm/sec). For a transmitted signal bandwidth of 2 MHz, the longitudinal resolution ΔR is about 0.375 mm.

The above results demonstrate the independence of velocity resolution and range resolution, and indicate that they are only limited by bandwidth considerations. The important concept is that the bandwidth of the transmitted signal (B) and the bandwidth of the filter following correlation (W) can be controlled independently, thereby making it possible to make very accurate range and velocity measurements simultaneously.

The remaining essential characteristic of the ultrasonic system to be considered is the efficiency with which weak return signals can be detected. This is most conveniently done in terms of examining the output signal-to-noise ratio as a function of the parameters of the system. The output signal-to-noise relationship for an ultrasonic system in which the correlation operation is continuous is given by [58]

$$(S/N)_o = \left[\frac{p_t G^2 \lambda^2 \sigma}{(4\pi)^3 R^4 k T B_r F_r}\right] \cdot \left[\frac{B}{W}\right] \qquad (14)$$

where p_t is the transmitted power, G is the antenna gain, λ is the wavelength, σ is the echoing area, R is the range, k is Boltzmann's constant, T is the ambient temperature B_r is the receiver bandwidth, F_r is the receiver noise figure, B is the bandwidth of the transmitted signal, and W is the bandwidth of the bandpass filter. The first factor in equation 14 is simply the signal-to-noise ratio at the receiver input while the second factor is the increase in the signal-to-noise ratio due to correlation processing. This increase is typically greater than 20 times.

So far the theoretical performance of the random signal ultrasonic system performing continuous correlation has been considered. This, however, does not represent a practical procedure because of the difficulty of obtaining large, continuous delays over the bandwidths required. Hence a practical implementation requires that the reference and received signals be sampled prior to correlation and that the delay be obtained digitally. The analysis has been extended to consider the effects of digital correlation [60,62]. It is shown that the output signal-to-noise ratio for a system using polarity coincidence correlation can be written as

$$(S/N)_o = \left[\frac{P_t G^2 \lambda^2 \sigma}{(4\pi)^3 R^4 kTB_r F_r}\right] \left[\frac{2f_s}{\pi^2 W}\right] \tag{15}$$

Again the first factor of equation 15 is simply the signal-to-noise ratio at the receiver input while the second factor is the increase due to correlator processing. The signal-to-noise ratio of the random signal system can be enhanced substantially by increasing the sampling rate f_s and/or by choosing a narrow filter bandwidth W.

Now that the theory of the random signal ultrasonic system has been discussed, it is appropriate to consider the characteristics that are significant in making biomedical measurements. These are summarized in the following section.

2.4 Characteristics and Advantages of the Random Signal System

1. The velocity resolution is determined by the bandwidth of the correlator output filter (W) and can be controlled independently of the transmitted signal bandwidth (B).

2. The range resolution is inversely proportional to the bandwidth of the transmitted signel (B). Since the transmitted pulses are samples of wideband Gaussian noise, the bandwidth can be varied to achieve the desired range resolution without shortening the pulse width. Thus, arbitrarily good range resolution can be achieved without resorting to pulse compression techniques.

3. The duty factor can be kept large thereby providing a greater average power for a given peak power.

4. The generation of random signals with large time-bandwidth products is usually easier than the generation of comparable deterministic signals.

5. Because of the pulse-to-pulse independence of the transmitted random waveform, there is no ambiguity

in range. Thus more than one pulse may occupy the transducer-to-target space at the same time without the possibility of obtaining false range measurements.

The problem of ambiguous return is a severe limitation to the use of conventional pulse-Doppler systems. This is due to the fact that the maximum unambiguous range and maximum unambiguous velocity are inversely related. Their product is a constant given by [55]

$$V_m \cdot R_m = \frac{c^2}{8f_c} \tag{16}$$

where V_m is the maximum unambiguous velocity, R_m is the maximum unambiguous range, f_c is the transmitted ultrasonic frequency and c is the velocity of ultrasound in the medium.

It can be shown that for f_c = 5 MHz and the desired maximum blood velocity of 100cm/sec a conventional pulse-Doppler ultrasonic system has a maximum unambiguous range of about 5.6cm. It is clear that this limits the application of conventional pulse systems in studying blood flows in deep-lying vessels.

Similarly, range and velocity ambiguities may occur in ultrasonic systems which transmit pseudo-random binary sequences because of the periodic nature of these signals. However the proposed random signal system transmits non-periodic signals and hence, there are no range ambiguities.

6. Because there are no range ambiguities, the pulse repetition rate can be made sufficiently high to measure any given Doppler shift unambiguously in the absence of clutter. Thus, spectrum folding which might otherwise occur with high velocity targets, is completely avoided.

7. Since the correlator performs coherent detection, all Doppler shifts appear at the output with their correct relative frequencies and can be extracted by simple band-pass filters.

8. The output signal-to-noise ratio for the proposed system will be considerably higher than for the existing pulse-Doppler ultrasonic systems. This is due to several inherent advantages of the random signal processing technique. The improvement in the signal-to-noise ratio can be accomplished in the following ways:

a. By increasing the sampling rate f_s and/or by choosing a narrow bandwidth W of the filter following the digital correlator (see equation 15).

b. By transmitting a random signal having an average power many times larger than could be obtained from a conventional pulsed signal with the same peak power.

c. By integrating a large number of consecutive output pulses. It is known that for n integrated pulses, the signal-to-noise ratio is improved by a factor n for coherent integration or by a factor $\sqrt{n}$ for non-coherent integration [63]. In conventional pulse-Doppler systems it is not possible to integrate a large number of output pulses without destroying the range information. In the random signal system, coherent integration of several thousand pulses may be easily accomplished by simply increasing the observation time of the system. This is achieved by changing the bandwidth of the filter following wideband correlation, since the observation time of the system is inversely related to the bandwidth of this filter (W).

From the above discussion it is clear that considerable signal-to-noise ratio enhancement can be achieved by the random signal ultrasonic system. Therefore it should be possible to make transcutaneous measurements of blood flows in deep-lying vessels which are presently unaccessible with existing pulse-Doppler techniques.

2.5 Limitations of the Random Signal System

1. In a continuous clutter environment with the target distributed over a large range interval, the random signal may return more clutter power than a deterministic signal, unless its duty factor is made equally small [58].

2. With a practical polarity coincidence correlator, amplifier non-linearities, sampler voltage offsets and other

effects may cause the polarity decisions to be made on an offset version of the input signals. However it does not appear that these reference level errors will be a significant limitation to the performance of a practical correlator since adjustments can be made to reduce these errors [62].

3. Although there is no fundamental loss in detectability with stochastic signals, the random signal ultrasonic system has the disadvantage of requiring amplifiers and receivers with larger power bandwidths.

2.6 General Description of the System

The block diagram of Figure 5 shows one way to implement the operations of the random signal ultrasonic system described in the previous sections. The random signal to be transmitted is generated by a noise source which is followed by a variable bandpass filter. This filter has a nominal bandwidth of 4 MHz centered at a midband frequency of 5 MHz. By varying the bandwidth of this filter it is possible to adjust the range resolution of the system (equation 13). A gating circuit follows the bandpass filter to adjust the on-off ratio of the transmitted signal. The optimum value of the duty factor can be calculated for a given clutter environment surrounding the living tissue under examination.

The gated signal is then amplified. A portion of this signal is extracted and used as a reference. The rest of the signal is converted from an electrical to an acoustic

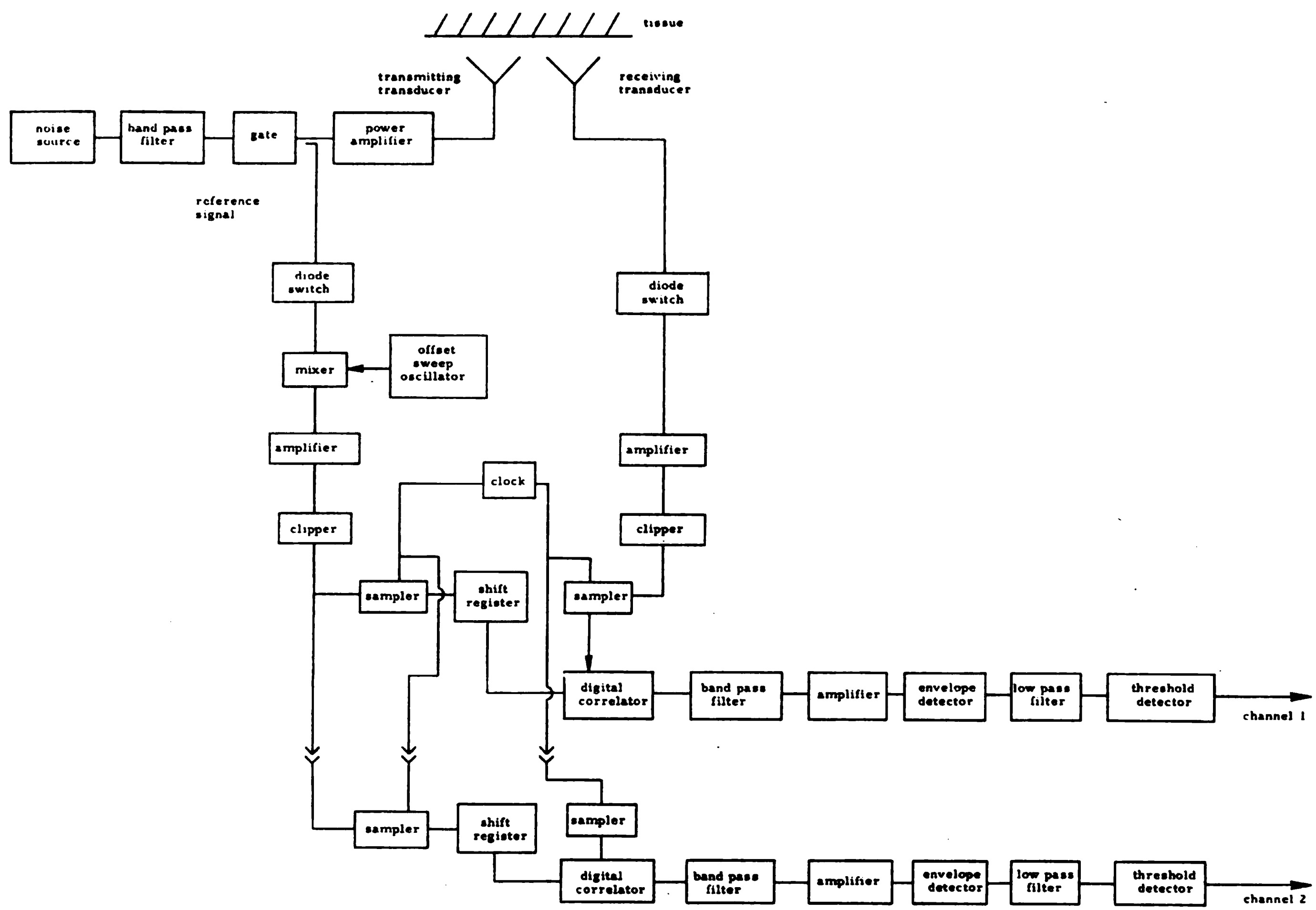

Figure 5.--Diagram of the Complete Random Signal Ultrasonic System.

waveform by a piezoelectric transducer which acts as a transmitter, and is aimed at the living tissue. The reflected acoustic signal is converted back to an electrical signal by the receiving piezoelectric transducer. A single ultrasonic transducer is normally adequate for both transmission and reception of pulsed signals if an appropriate decoupling network is utilized.

Both the reference and received signals are amplified, clipped to retain only polarity as is done in random signal microwave radar [58-61], and sampled with a very short pulse. The local oscillator for the reference channel mixer is offset in frequency a small amount of the order of the maximum Doppler shift expected. This offset makes it possible to set the frequency of the correlator output for zero velocity targets to any desired value (so that bandpass rather than lowpass filtering can be used.) Also, it eliminates the ambiguity between Doppler shifts for approaching and receding targets.

The necessary delay between the reference and received signals is accomplished by a combination of discrete and continuous delays. The discrete delay consists of a shift register which delays the binary samples in the reference channel by any desired integral number of sampling periods. The continuous delay is accomplished by adjusting the sampling time for the receiver channel within the interval of one sampling period. Binary sequences for the reference channel and the receiver channel are cross-correlated in a digital "exclusive-OR" circuit followed by an inverter.

The correlator output consists of a digitized random signal that contains the Doppler frequency shifts of the target as shown in Figure 6b. This digitized signal is averaged by a bandpass filter which selects the Doppler frequencies of interest. It is the bandwidth W of this filter that determines the velocity resolution (equation 12), and performs the coherent integration.

The filter output is then envelope detected and low-pass filtered to create the signal used for the display. To observe the output of n different ranges, the correlator may be slowly swept in range, requiring a total observation time which is n times long. An alternative is to use n parallel correlators, as shown in Figure 5, for a corresponding decrease in observation time and increase in equipment complexity.

The output of the low pass filter may be displayed in two different modes. In the first mode, shown in Figure 6c, the velocities are displayed as a function of range. The range sweep is accomplished by varying the delay provided by the shift registers. It is hoped that this display will allow the experienced investigator to orient the transducer placement.

Figure 6.--Waveforms Associated With Blood Velocity Measurements.

a. Transmitted waveform.

b. Time averaged correlator output.

c. Velocity versus range for many heart beats.

d. Velocity versus time at a given range.

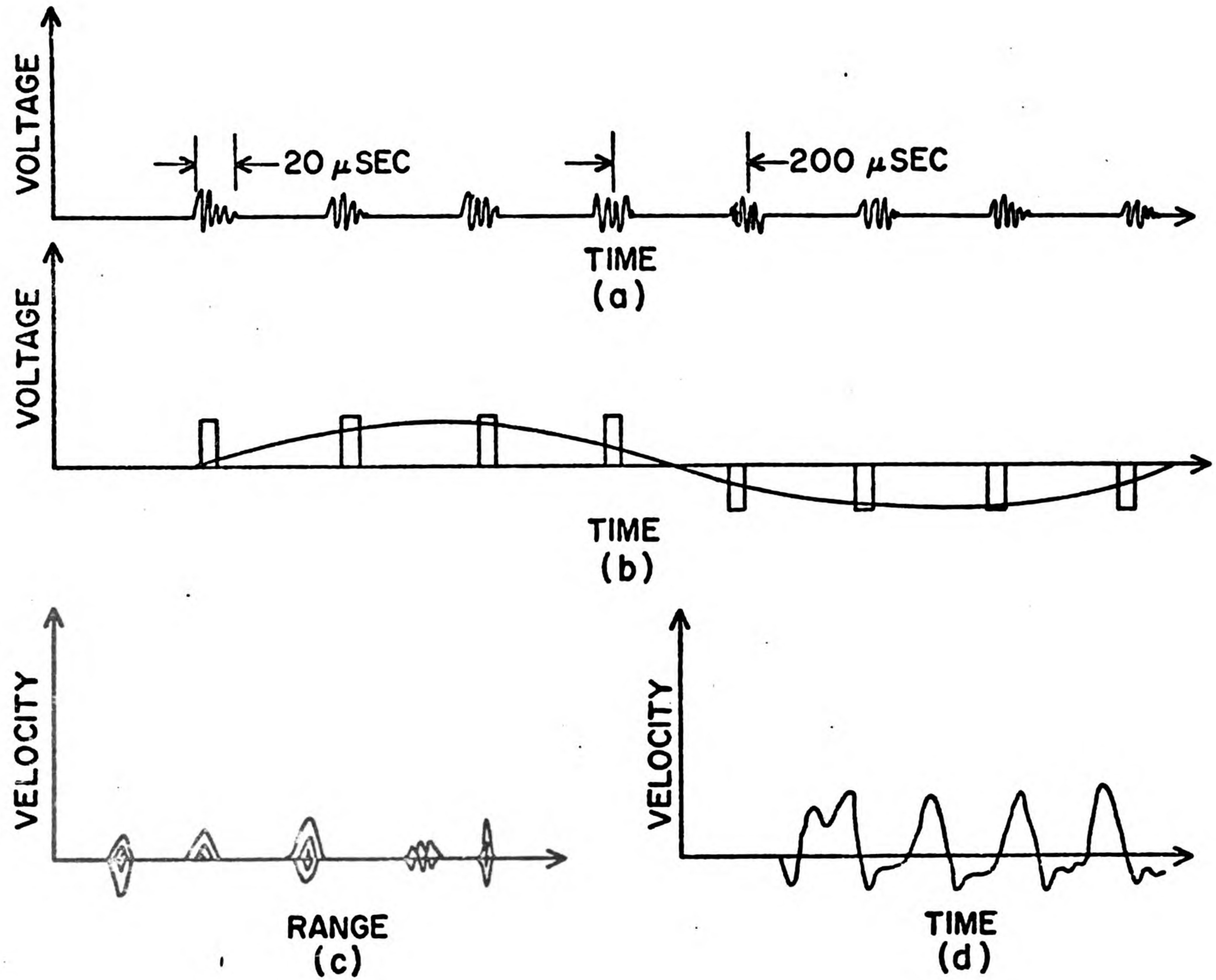
VOLTAGE
20 μSEC
200 μSEC
TIME
(a)
VOLTAGE
TIME
(b)
VELOCITY
RANGE
(c)
VELOCITY
TIME
(d)

Figure 6.

Once orientation has been achieved, the investigator can switch to the second mode of display shown in Figure 6d. Here velocity is depicted as a function of time at a specific range. The entire system may also be synchronized with an electrocardiogram to provide additional information.

CHAPTER III

EXPERIMENTAL RANDOM SIGNAL ULTRASONIC SYSTEM

3.1 System Implementation

A simplified version of the random signal ultrasonic system described in Chapter II has been built and results have been obtained for the Doppler resolution. The block diagram of the experimental system is shown in Figure 7.

3.1.1 Circulation Model

Figure 8 is a photograph of the circulation system used to simulate blood flow. Polystyrene particles of size 50-75 microns are mixed in water and circulated in the tygon tube by using a peristaltic pump. The flexible tygon tube is connected to a section of glass tubing which passes through the water tank. This glass tubing corresponds to a blood vessel with an inside diameter of 8mm and a wall thickness of 0.5mm.

The transducers used for transmitting the ultrasonic pulses and detecting the Doppler frequency shifted echoes are positioned directly over the glass tube. Each transducer

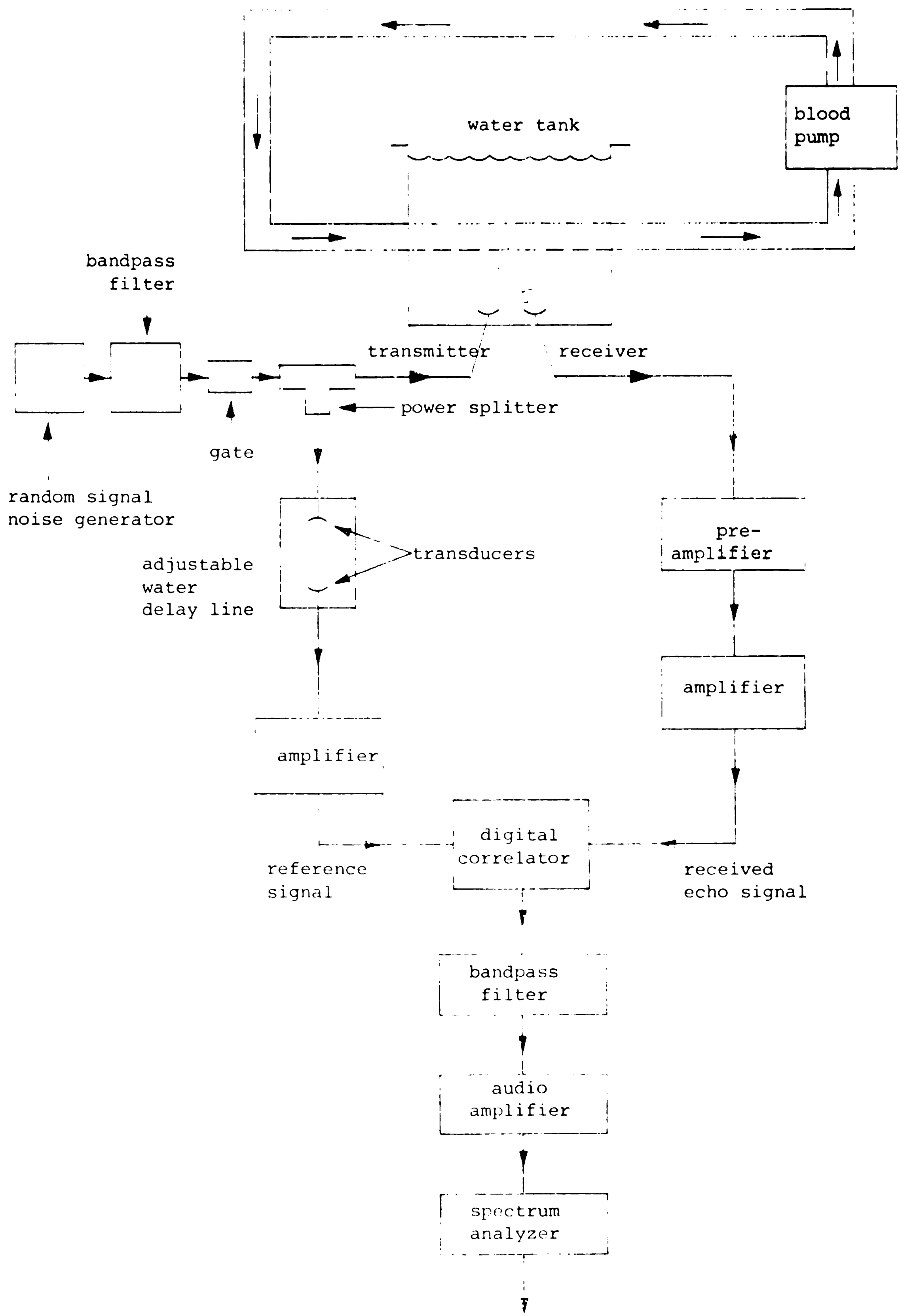

Figure 7.--Simplified Experimental System.

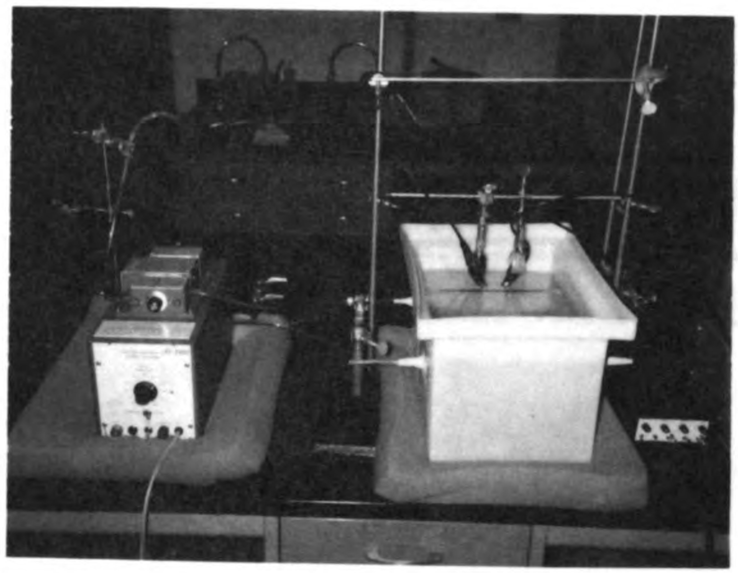

Figure 8.--Circulation System.

face is separated from the centerline of the tube by a nominal distance of 3 centimeters. These piezoelectric transducers will be discussed in section 3.1.3.

For the given tube diameter (8mm ID), the variable speed peristaltic pump is capable of moving the polystyrene particles over a continuous velocity range from 0-40 cm/sec. These particles circulate best at velocities above 10 cm/sec, due to their large size and corresponding weight.

As shown in Figure 8 the bases of both peristaltic pump and polyethylene water tank are insulated with foam cushions to minimize the environmental vibrational effects.

3.1.2 Transmitter

The transmitter subsystem consists of the following:

1. A random signal noise generator
2. A bandpass filter
3. A transmission gate
4. A linear power amplifier and power splitter.

The random signal noise generator uses a gas discharge tube as its noise source. The noise output from the gas tube is amplified in a two stage amplifier before being input to the active bandpass filter.

The two-pole bandpass filter has a center frequency $f_c = 4.59$ MHz and a bandwidth of 4 MHz. An operational amplifier is inserted after the bandpass section to provide an additional 7dB signal gain.

The filtered noise is limited to pulses 10μsec wide by means of a linear transmission gate. The pulse repetition frequency (PRF) is approximately equal to 10 KHz. The gate has been fixed at 10μsec although other durations are possible.

A broadband solid state power amplifier covering the frequency range of 250 KHz to 110 MHz is used to amplify the gated signal. A nominal gain of 50dB raises the random noise pulse to approximately 120 volts peak-to-peak. A BNC tee connector acts as the power splitter shown in Figure 7. The amplifier output is used to drive the two piezoelectric transmitting transducers. The need for two transmitting transducers will be discussed in the subsequent sections.

3.1.3 Transducers

The experimental system uses single element broadband transducers. These piezoelectric transducers have a low Q which makes them suitable for pulse-echo operation. Separate transducers are used for transmitting and receiving the random signals to avoid the problem of decoupling the transmitter from the receiver.

Referring back to Figure 7, there are two transmitter and receiver transducer pairs. One set of transducers is used to generate the delay between the reference signal and the received signal echoes. This arrangement will be discussed in the next section. The other transducer pair is used to detect the Doppler signals. This latter arrangement is shown in Figure 9.

The transmitting and receiving transducers used for sensing the motion of the polystyrene particles are positioned directly over the simulated blood vessel. The transducer faces are immersed in a water bath to provide the acoustic coupling necessary for the transmission and reception of ultrasound. Each transducer face is separated from the centerline of the vessel by a nominal distance of 3 centimeters. The angles α and β associated with the calculation of the fluid velocity (see equation 2) are measured directly with a protractor.

3.1.4 Adjustable Delay Line

The necessary delay between the reference and received signals is obtained by an adjustable analog delay line, rather than by sampling and using digital shift registers. The analog delay line, consisting of a water tank and two piezoelectric transducers, is shown in Figure 10. The variable delay of the reference signal is achieved by keeping the transmitting transducer fixed and moving the receiving reference transducer.

For a velocity of sound in water of approximately 1.48×10^5 cm/sec, the range factor is 13μsec of delay per

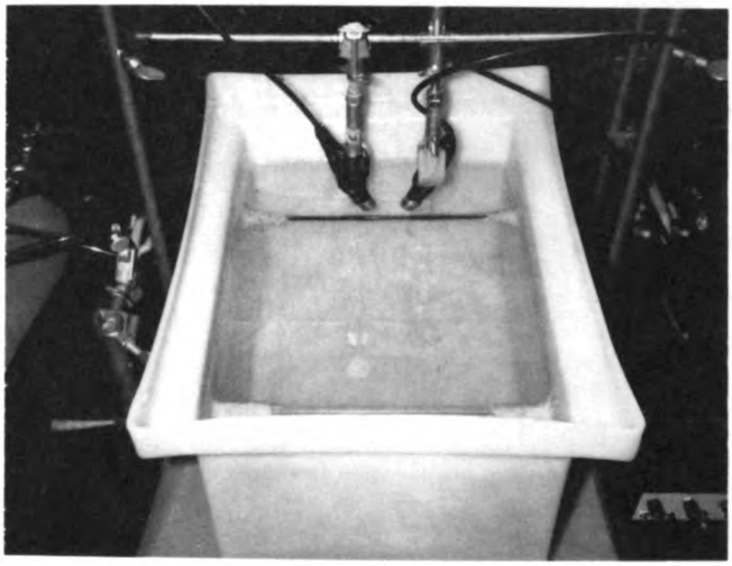

Figure 9.--Transducer Arrangement For
Doppler Detection.

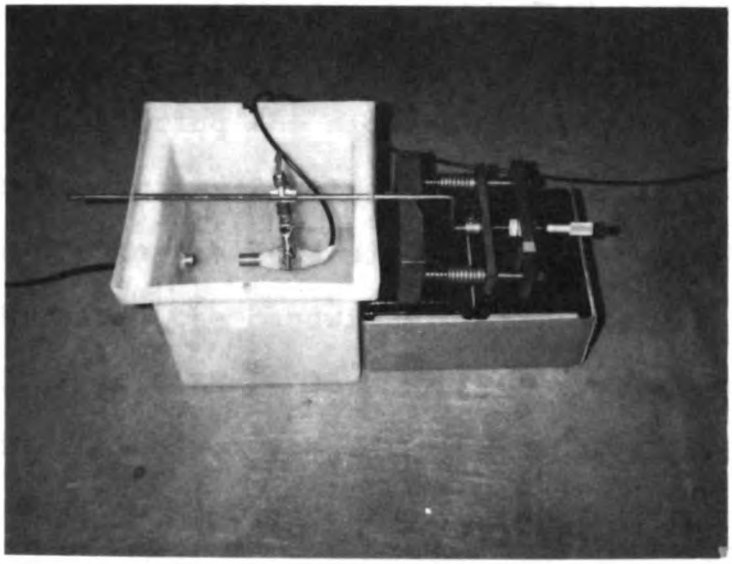

Figure 10.--Adjustable Analog Delay Line.

centimeter. The dimensions of the water tank therefore allow a maximum delay of 115μsec between the reference signal and the Doppler shifted signal.

3.1.5 Receivers

Referring to Figure 7 again, both reference signal and received signal are passed through high frequency amplifier sections to bring the signals up to a suitable level for cross-correlation (2 volts peak-to-peak.)

The Doppler shifted signal is increased by a gain of 60dB. Although the bandwidth of the preamplifier is close to 35 MHz (10 KHz - 35 MHz), the overall receiver bandwidth is limited to 6 MHz (2-8 Mhz) by the second-stage amplifier. The noise figure for the overall receiver section is approximately 12dB.

Due to the relatively high level of the reference signal available, an increase in gain of 40dB brings the reference channel up to a suitable level for correlation. The reference channel's amplifier section has a bandwidth of 35 MHz and a noise figure less than 8dB.

3.1.6 Correlator

The correlator subsystem consists of the following:

1. A digital correlator
2. A bandpass filter
3. An audio amplifier.

The digital correlator is simply an "exclusive-OR" logic circuit followed by an inverter. In this case, the correlator performs a multiplication of the reference signal with the received signal. This logic circuit produces a coincidence output when the two inputs agree and an anti-coincidence output when they are different.

The correlator output consists of a digitized random signal that contains the Doppler frequency shift of the moving target. In addition to the Doppler frequency shift, there are signals due to spatial leakage changes that extend down to DC and are large in amplitude [5]. These leakage components vary widely when the transducers are moved intentionally or from random motion. In the experimental random signal system, a 4-pole active bandpass filter with unity gain follows directly from the correlator output. This filter has a variable bandwidth to reject the spatial leakage components and select the Doppler frequency of interest. Coherent integration is also performed by the filter.

An audio amplifier with a bandpass exceeding the maximum filter bandwidth follows. The Doppler signal is raised to a suitable level for display on the spectrum analyzer.

Figure 11 is a photograph of the complete experimental system.

Figure 11.--Photograph of the Experimental System.

3.2 Doppler Resolution Results

An indication of the Doppler resolution of the experimental system is given in Figures 12-15. The test was performed by aligning the transmitting and receiving transducers directly over the glass vessel as shown previously in Figure 9. The necessary delay between the reference and received channels was manually adjusted to correspond to observations made in the center of the tube. Significant parameters associated with the experimental system are given in Table 1.

Figure 12 shows the correlator output after bandpass filtering and audio amplification with the polystyrene particles stationary. This is the frequency domain representation of the background noise.

Figures 13-15 represent the Doppler resolution obtained with the polystyrene particles moving at various speeds. As the velocity of the particles is increased, the dominant Doppler shift frequency is seen to increase. The bandwidth of the filter following correlation was adjusted to select the frequency range of interest.

Prior to these experiments, the various velocities of the polystyrene particles were measured by external means and these values used to calculate the theoretical Doppler frequency shifts. A comparison of the theoretical Doppler frequency shifts expected and the experimental frequency shifts observed are presented in Table 2.

TABLE 1.--Characteristics of the Experimental System

Transmitted center frequency f_o	4.59 MHz
Transmitted random frequency bandwidth	4 MHz
Pulse width	10μsec
Pulse repetition rate	10 KHz
Delay	78μsec
Receiver noise figure	12dB
Receiver gain	60dB
Transducer arrangement:	
Distance between transmitting transducer and vessel centerline	3cm
Distance between receiving transducer and vessel centerline	3cm
Angle α between transmitted ultrasonic beam and velocity vector	65^o
Angle β between received ultrasonic beam and velocity vector	115^o

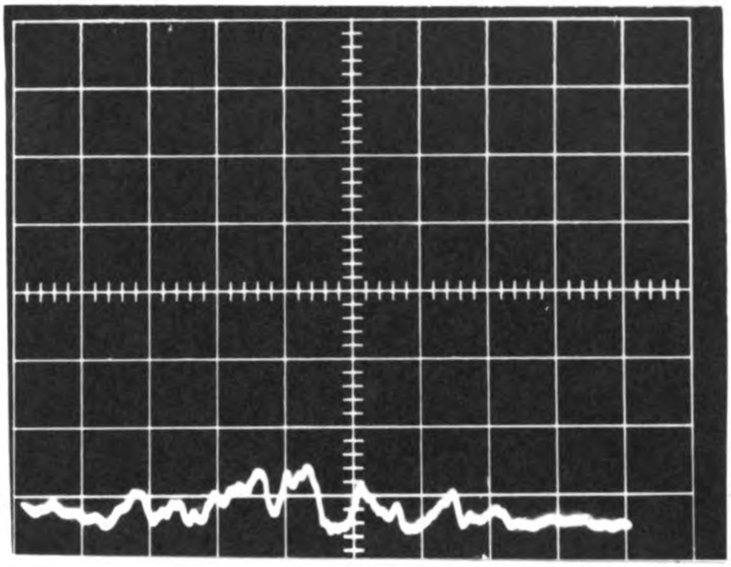

Frequency display range	0 - 2000 Hz
Horizontal scale	200 Hz/cm
Vertical scale	2v/cm
Correlator filter bandwidth	400 - 2000 Hz

The polystyrene particles are stationary.

Figure 12.--Frequency Domain Representation of Background Noise.

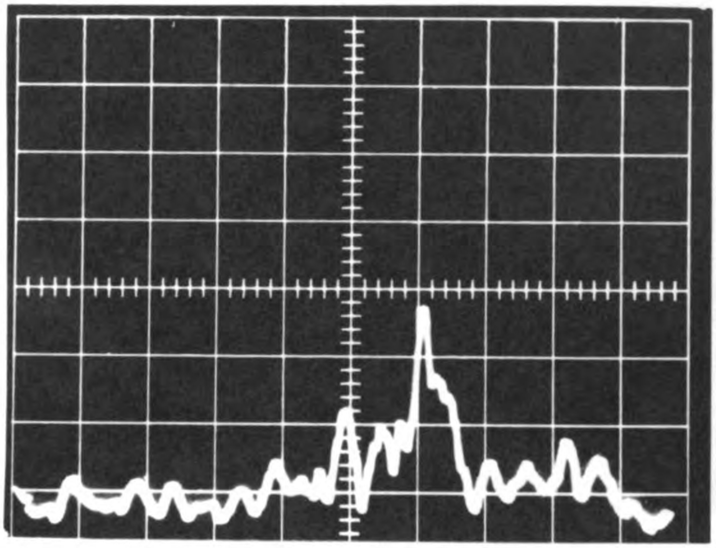

Frequency display range	0 - 1000 Hz
Horizontal scale	100 Hz/cm
Vertical scale	2v/cm
Correlator filter bandwidth	400 - 800 Hz
Pre-determined velocity of particles	23.4 cm/sec
Doppler frequency:	
a) observed	620 Hz
b) theoretically calculated	614 Hz

Figure 13.--Doppler Resolution.

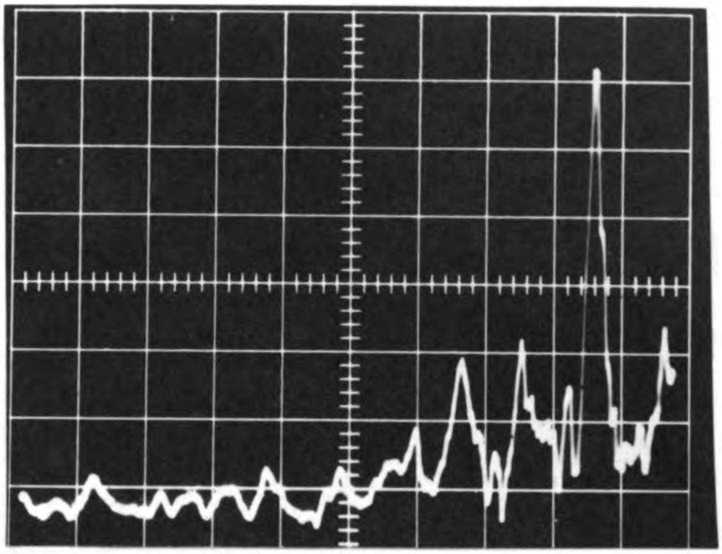

Frequency display range	0 - 1000 Hz
Horizontal scale	100 Hz/cm
Vertical scale	2v/cm
Correlator filter bandwidth	500 - 1250 Hz
Pre-determined velocity of particles	33.7 cm/sec
Doppler frequency:	
a) observed	870 Hz
b) theoretically calculated	878 Hz

Figure 14.--Doppler Resolution.

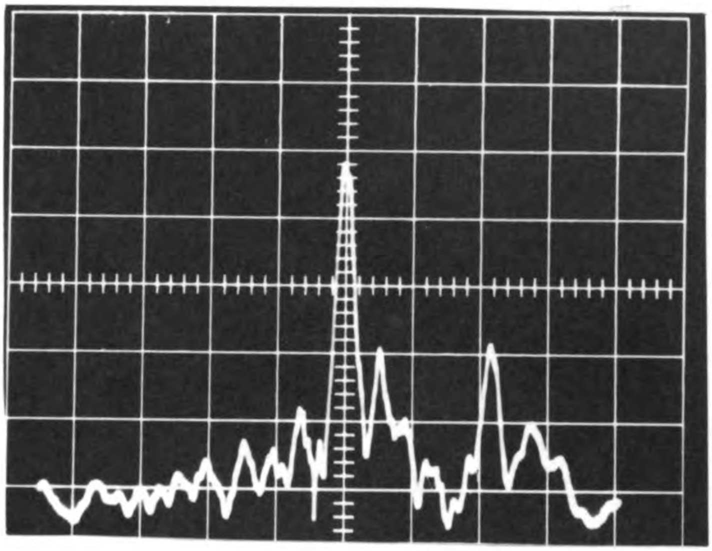

Frequency display range	0 - 2000 Hz
Horizontal scale	200 Hz/cm
Vertical scale	2v/cm
Correlator filter bandwidth	630 - 1250 Hz
Pre-determined velocity of particles	39.1 cm/sec
Doppler frequency:	
a) observed	1000 Hz
b) theoretically calculated	1021 Hz

Figure 15.--Doppler resolution.

TABLE 2.--Comparison of Theoretical Doppler Frequencies Expected and Experimental Doppler Frequencies Observed

Calibrated Particle Velocity at Tube Centerline	Theoretical Doppler Frequency Shift	Experimental Doppler Frequency Shift
23.4cm/sec	614 Hz	620 Hz
33.7cm/sec	878 Hz	870 Hz
39.1cm/sec	1021 Hz	1000 Hz

Formula used for calculation of the theoretical Doppler shift frequency fd:

$$f_d = \frac{f_o}{c}\,[\cos\alpha - \cos\beta] \cdot v \qquad (17)$$

where $c = 1.48 \times 10^5$cm/sec

$f_o = 4.59$ MHz

$\alpha = 65^o$

$\beta = 115^o$

velocities v are given in the table above.

3.3 Conclusions

The theoretical and experimental Doppler results outlined above leave no doubt that it is entirely feasible to build pulsed ultrasonic systems employing stochastic signals. An analysis of the results presented in Table 2 indicate that the experimental random signal ultrasonic system is capable of measuring the Doppler difference frequency within an error range of $\pm$ 1%.

CHAPTER IV

THEORY AND OPERATION OF A DUAL ELEMENT BROADBAND TRANSDUCER

4.1 Introduction

An increase in longitudinal and lateral resolution is required in order to apply pulsed Doppler ultrasonic blood flow techniques to deep-lying and small blood vessels. In Chapter II it was theoretically shown that the range (longitudinal) resolution ΔR of a random signal ultrasonic system is approximately c/2B, with c the velocity of ultrasound in the medium and B the bandwidth of the transmitted signal. Using a system similar to that described in Chapter III, with a noise center frequency of 5.8 MHz and a transmitted signal bandwidth of 2 MHz, Newhouse et al. [64] confirmed the predicted range resolution $c/2B \simeq 0.35$mm. The target was a stationary steel ball in water. It was also shown that the range (along-the-beam) resolution could be made arbitrarily sharp or coarse by varying the signal bandwidth B.

The lateral resolution, which is in a direction perpendicular to the ultrasonic beam axis. depends upon the dimensions of the transducer face. This resolution may be improved by focusing the ultrasonic beam with lenses. However, this technique increases the complexity of the system and is accompanied by the attended risk of generating acoustic intensities harmful to living tissues. To circumvent these difficulties a novel broadband dual element transducer [67] was developed by Doctor C. P. Jethwa of Michigan State University in collaboration with the Panametrics Company.

4.1 Principle of Operation

The basic principle involved in the operation of the dual element transducer can be explained by considering a transmitting element T surrounded by eight receiving elements $R_1 - R_8$ as shown in Figure 16a. Figure 16b shows that if the target is directly ahead of the transmitting element T such as target 1, the cone of the reflected acoustic energy will arrive at all receivers $R_1 - R_8$ at precisely the same time. The signal detected by each receiver will be added together since receivers $R_1 - R_8$ are connected in series. The resultant signal will be quite large because the eight receivers are in phase with each other.

If however, the target is at an angle to the centerline of the transmitted beam such as target 2 in Figure 16b, the reflected signal will arrive at each receiving element $R_1 - R_8$ at a different time with the result that some of the

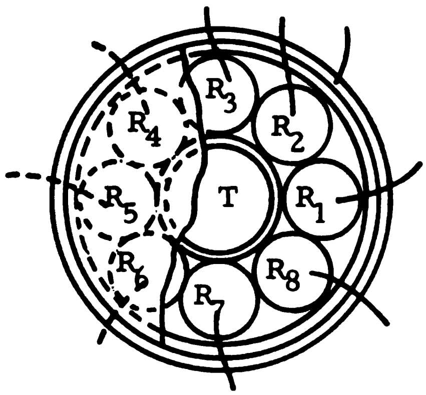

(a)

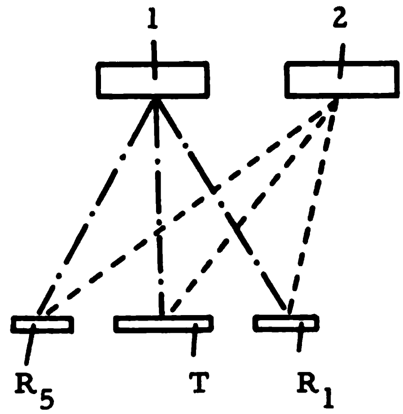

(b)

Figure 16.--Construction of the Dual Element Wideband Ultrasonic Transducer.

receivers will be out of phase with respect to each other. The integrated sum of the several receivers $R_1 - R_8$ is accordingly much reduced.

The dual element broadband transducer reported in this thesis has a Q of 2.5, a transmitting diameter of 1.26 cms., and an annular receiver diameter of 1.9cms. In this transducer a single annular ring is used as a receiver in place of the eight receiving elements. However the basic principle of operation remains the same.

Although ultrasonic transducers with similar coaxial configurations have been reported [65,73,74], they are primarily used for continuous-wave single frequency operation. Hence their construction is drastically different from the transducer reported here which operates in the broadband pulsed mode. Also lateral resolution data for these transducers has not been reported.

4.3 Experimental Results and Conclusions

In this section the dual element wideband transducer is compared to a single element broadband transducer in terms of lateral resolution capability. In order to determine the lateral resolution, the following experiment was devised. A 1.5cm diameter steel ball was held stationary in a water bath. The transducer being tested was mounted in a scanning device and aimed directly at the spherical target.

While operating in the pulse-echo mode, the transducer was moved laterally to scan the target.

Figure 17 and Figure 18 show the amplitude of the echoes received by the single element transducer at various distances between the transducer face and target plane. Similar results for the dual element transducer are shown in Figure 19 and Figure 20. The half amplitude lateral resolution data obtained from these figures is plotted in Figure 21 for comparison. It can be seen that the lateral resolution of the dual element broadband transducer is markedly superior to that of the single element transducer.

It is expected that by combining the unique properties of random signal processing with the superior directional and sensitivity properties of the dual element transducer, it should be possible to develop a system capable of making blood flow measurements on deep-lying blood vessels and small blood vessels. A preliminary attempt was made to incorporate the dual element transducer into the experimental system described in Chapter III. However some modifications must be made on the receiver amplifier section before Doppler results can be obtained.

Figure 17.--Echoes Received by the Single Element Transducer Scanning the Target Laterally.

a. Water Path--5.1 cms.
Vertical Sensitivity--0.1V/div.
Horizontal Sensitivity--1.34 mm/div.
Attenuation--10 dB
Target--1.58 cms. dia. steel ball

b. Water Path--7.6 cms.
Vertical Sensitivity--0.1V/div.
Horizontal Sensitivity--1.34 mm/div.
Attenuation--10 dB
Target--1.58 cms. dia. steel ball

SINGLE ELEMENT BROADBAND TRANSDUCER
Center Frequency - 5 MHz, Bandwidth - 3 MHz
Diameter - 1.26 cms.

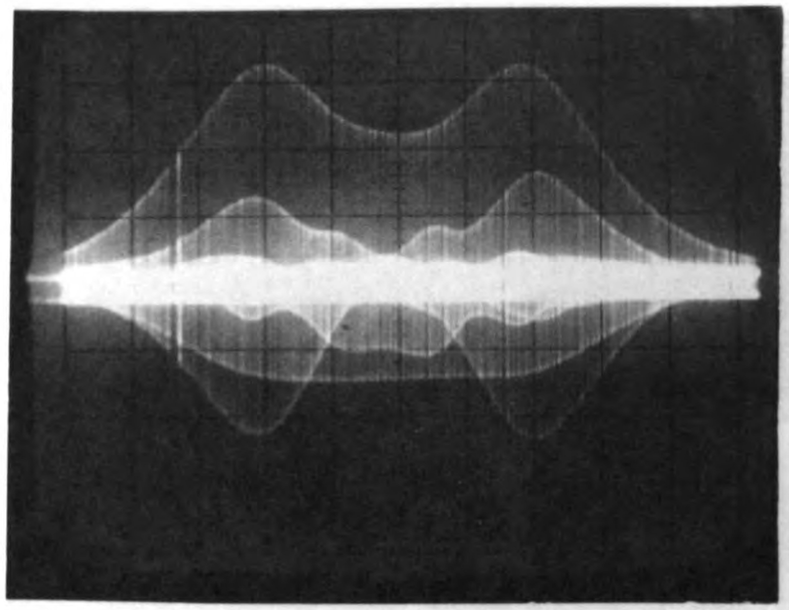

(a)

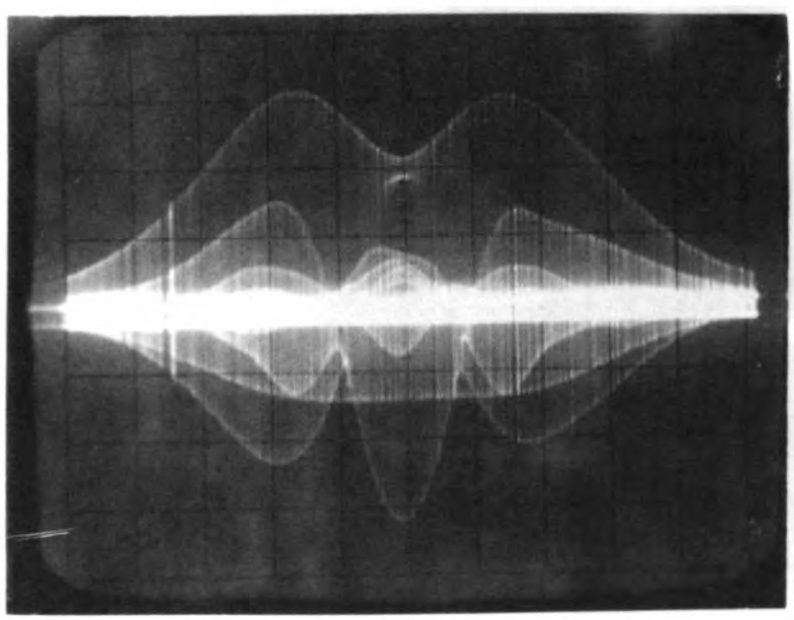

(b)

Figure 17.

Figure 18.--Echoes Received by the Single Element Transducer Scanning the Target Laterally.

a. Water Path--10.2 cms.
Vertical Sensitivity--0.2V/div.
Horizontal Sensitivity--1.34 mm/div.
Attenuation--10 dB
Target--1.58 cms. dia. steel ball

b. Water Path--12.7 cms.
Vertical Sensitivity--0.2V/div.
Horizontal Sensitivity--1.34 mm/div.
Attenuation--10 dB
Target--1.58 cms. dia. steel ball

SINGLE ELEMENT BROADBAND TRANSDUCER
Center Frequency - 5 MHz, Bandwidth - 3 MHz
Diameter - 1.26 cms.

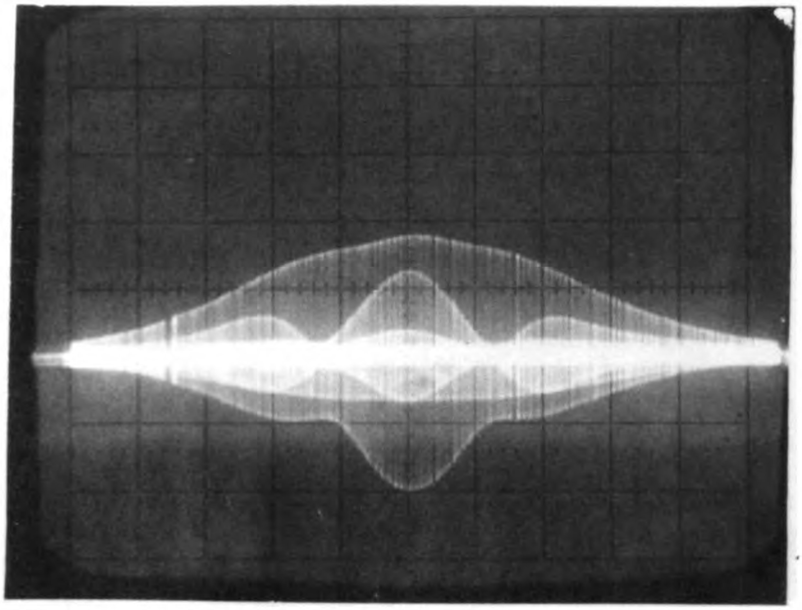

(a)

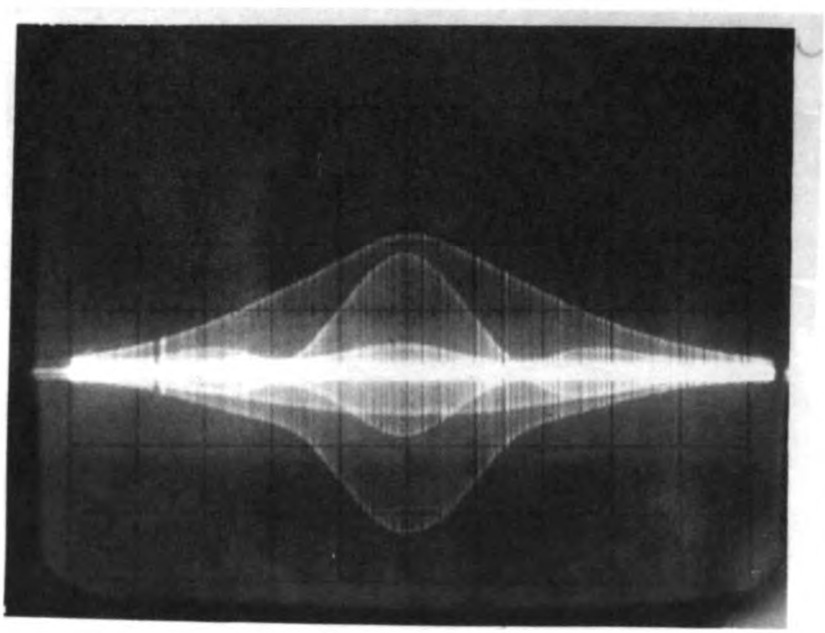

(b)

Figure 18.

Figure 19.--Echoes Received by the Dual Element Transducer Scanning the Target Laterally.

a. Water Path--5.1 cms.
Vertical Sensitivity--0.1V/div.
Horizontal Sensitivity--1.34 mm/div.
Attenuation--10 dB
Target--1.58 cms. dia. steel ball

b. Water Path--7.6 cms.
Vertical Sensitivity--0.1V/div.
Horizontal Sensitivity--1.34 mm/div.
Attenuation--10 dB
Target--1.58 cms. dia. steel ball

DUAL ELEMENT BROADBAND TRANSDUCER
Center Frequency - 5 MHz, Bandwidth - 3 MHz
Transmitter Diameter - 1.26 cms.
Annular Receiver Diameter - 1.9 cms.

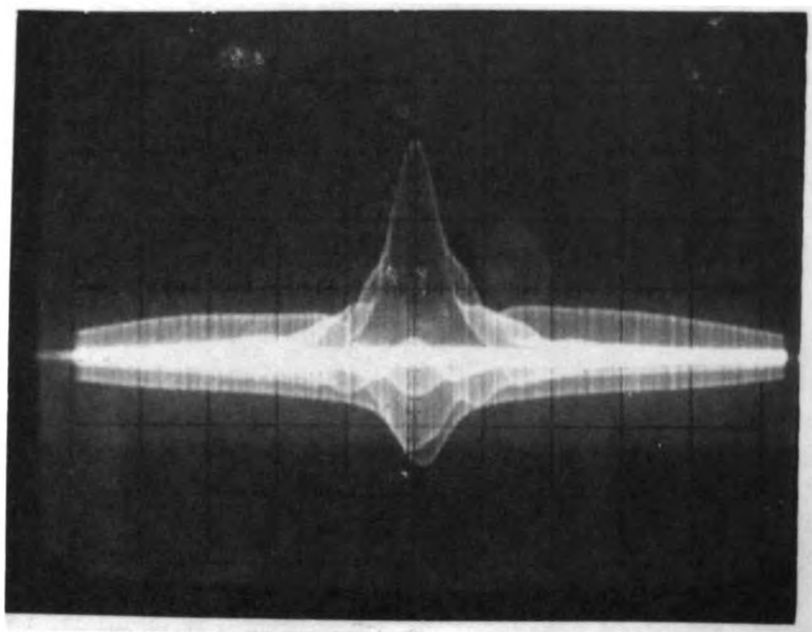

(a)

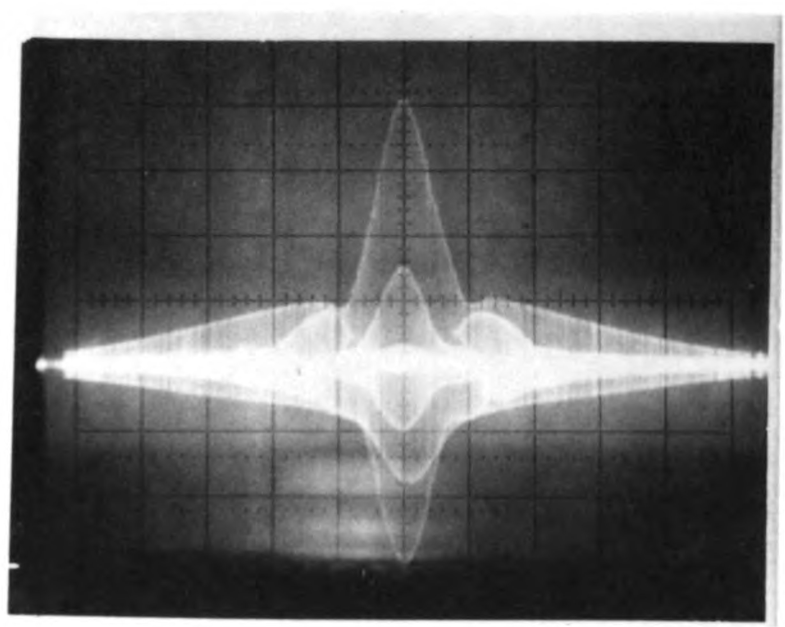

(b)

Figure 19.

Figure 20.--Echoes Received by the Dual Element Transducer Scanning the Target Laterally.

a. Water Path--10.2 cms.
Vertical Sensitivity--0.2V/div.
Horizontal Sensitivity--1.34 mm/div.
Attenuation--10 dB
Target--1.58 cms. dia. steel ball

b. Water Path--12.7 cms.
Vertical Sensitivity--0.2V/div.
Horizontal Sensitivity--1.34 mm/div.
Attenuation--10 dB
Target--1.58 cms. dia. steel ball

DUAL ELEMENT BROADBAND TRANSDUCER
Center Frequency - 5 MHz, Bandwidth - 3 MHz
Transmitter Diameter - 1.26 cms.
Annular Receiver Diameter - 1.9 cms.

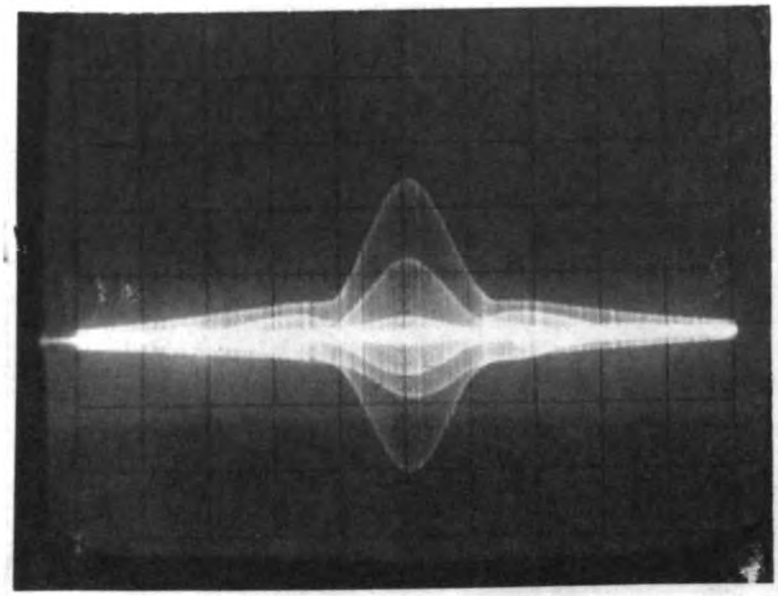

(a)

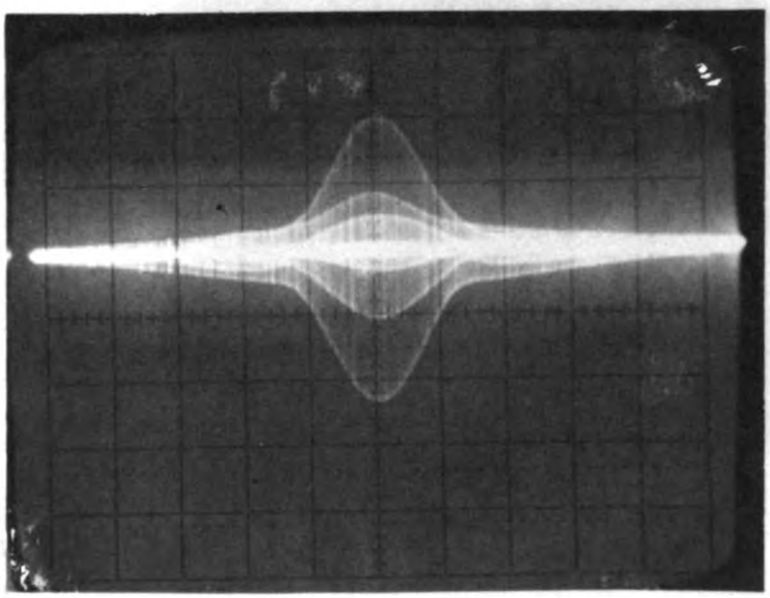

(b)

Figure 20.

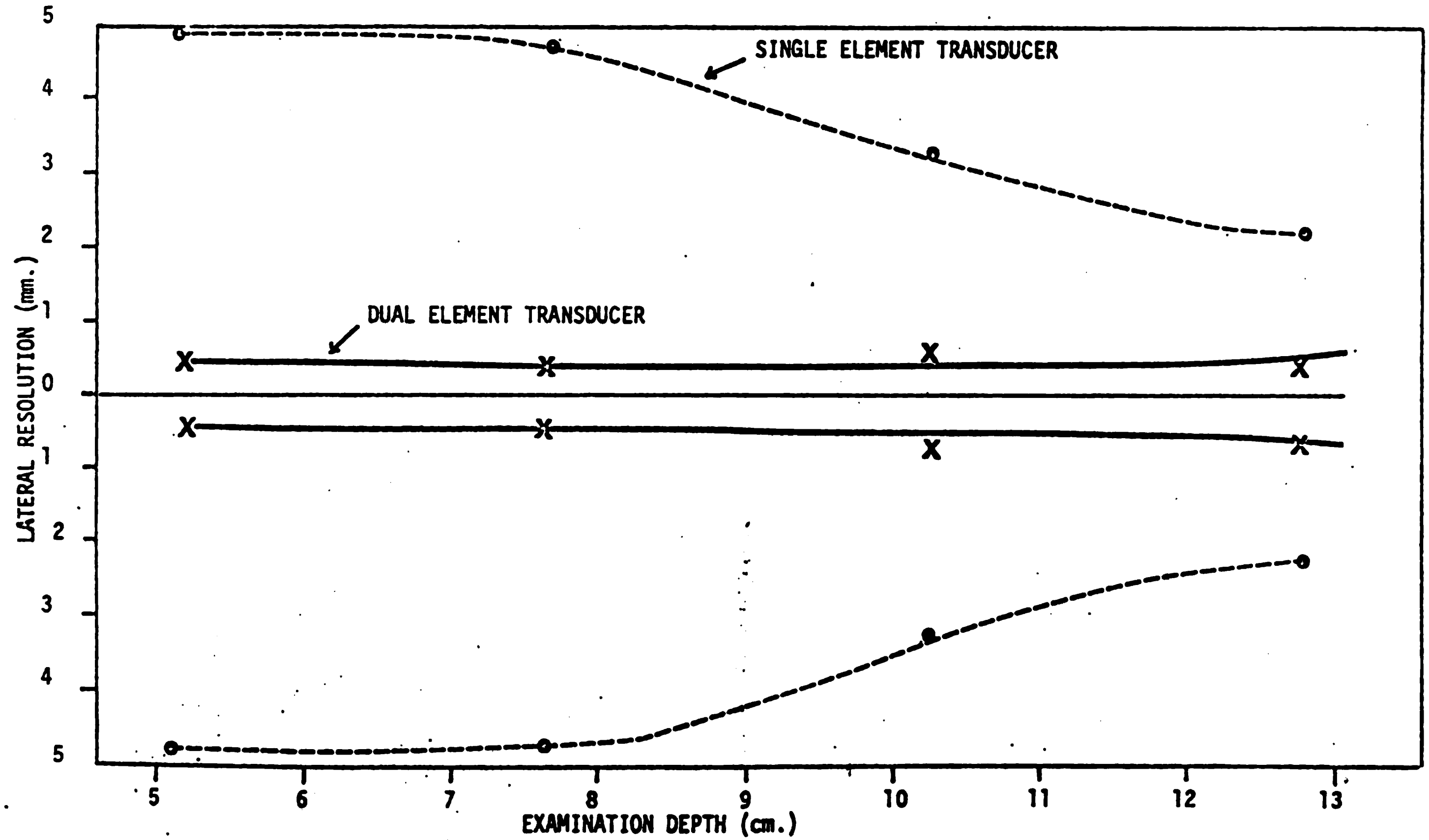

Figure 21.--Comparison of the Lateral Resolution of Single Element and Dual Element Transducers.

CHAPTER V

METHODS FOR DETERMINING THE ANGLES ASSOCIATED WITH DOPPLER BLOOD FLOW MEASUREMENTS

5.1 Introduction

Referring back to Chapter I the relationship between the average Doppler shift frequency f_d and the average blood flow velocity v was given by

$$v = \frac{c \cdot f_d}{f_o \cdot [\cos\alpha - \cos\beta]} \tag{18}$$

with c the velocity of ultrasound in blood, f_o the transmitted ultrasonic frequency, α the angle between the transmitted ultrasonic beam and the blood velocity vector, and β the angle between the received ultrasonic beam and the blood velocity vector.

When one transducer is employed as both transmitter and receiver the equation is modified in the following way.

$$v = \frac{c \cdot f_d}{2f_o \cdot \cos\theta} \tag{19}$$

where θ is the angle between the coincident transmitted and received ultrasonic beam and the blood velocity vector.

Although the random signal ultrasonic system described in Chapter II and Chapter III, and the novel transducer described in Chapter IV will enhance the detectability of blood velocity flow, an accurate determination of the ultrasonic angle of attack θ is necessary to quantify the in-vivo data. Baker [5] has stated that the determination of this angle is one of the two most important yet the most difficult parameter to measure. Paradoxically, the importance of this measurement is obscured by the fact that few techniques of angular calculation have been published.

This chapter examines two methods for calculating θ the ultrasonic angle of attack. The following techniques assume that one transducer is being used to both transmit and receive the ultrasonic pulses.

5.2 Oblique Triangulation Method

A definite procedure for measuring θ the sound beam angle has evolved. The transducer and theodolite holder [5] are positioned over the vessel with the initial angle between the skin surface and transducer less then 60°. The range to the near and far walls of the vessel are measured and the centerline range r_1 is computed. Next a vertical angle ϕ of 10° - 15° is turned in the direction toward normal to the vessel. If the vessel is straight, the near and far wall ranges of the vessel can again be measured and the centerline range r_2 computed.

An oblique triangle has now been constructed. θ is computed as the angle between sides r_1 and r, with side r_2 opposite the angle. Figure 22 illustrates this construction. The larger the angle ϕ, the more accurate will be the computation of θ. Other critical factors are the precision with which r_1 and r_2 can be calculated.

This method appears to be the accepted technique for calculation of the angle θ. However the most puzzling aspect is that the location of the vessel of interest beneath the skin is already presupposed. It seems hard to concede the availability of such information to the investigator except in the most limited circumstances.

The next technique examined exhibits a method by which both the location of the blood vessel and the angle of attack can be determined.

5.3 Compound B-scan Technique

5.3.1 Introduction

By using the information obtained from appropriate lateral and longitudinal B-scans, the blood vessel of interest can be located accurately beneath the skin and the angle of ultrasonic attack determined. A detailed analysis of the theory and operation of A-scope and B-scan techniques is beyond the scope of this thesis. The interested reader should consult the references given in the List of References [22,48].

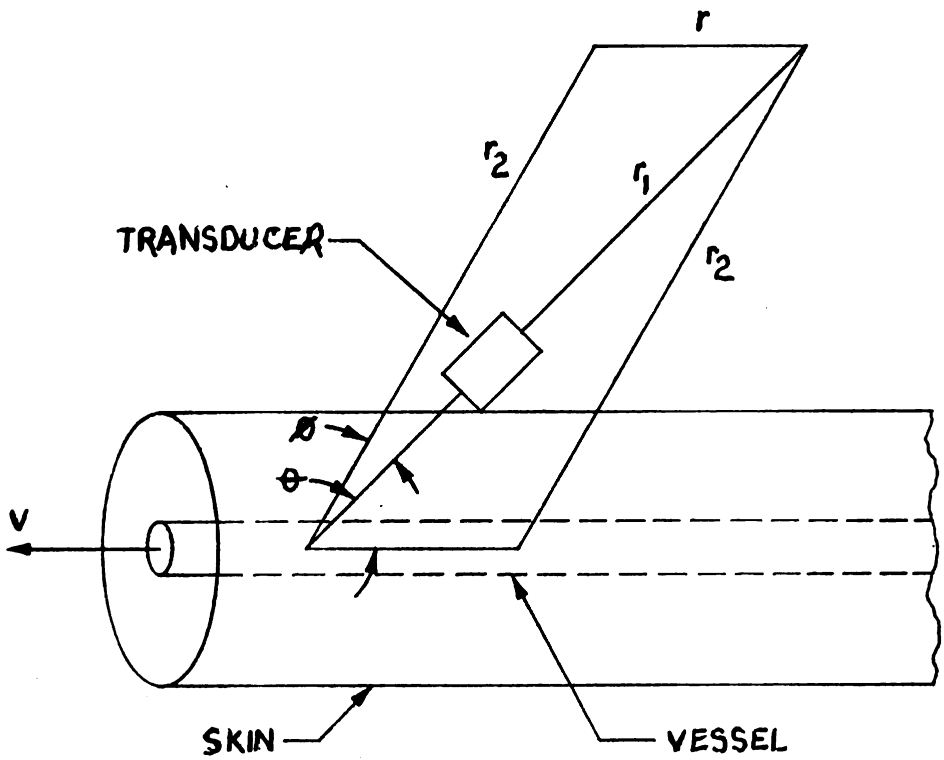

$$r = \sqrt{r_1^2 + r_2^2 - 2r_1r_2\cos\phi} \tag{20}$$

$$\theta = \cos^{-1}\left[\frac{r_1^2 - r_1r_2\cos\phi}{r_1\sqrt{r_1^2 + r_2^2 - 2r_1r_2\cos\phi}}\right] \tag{21}$$

Figure 22.--Oblique Triangle Construction.

5.3.2 Basic Principles

Figure 23 illustrates the A-scope and B-scope methods for displaying ultrasonic pulse-echo information. A schematic representation of a section through a patient is shown in Figure 23a. The interior circle represents the cross section of a typical blood vessel.

Pulse-echo systems which are used to measure the depth of an echo producing interface operate by the principle of ultrasonic wave reflection at tissue boundaries. When a transmitted ultrasonic pulse meets the boundary between two different media, a portion of the wave is reflected back through the incident medium. The time between transmission and reception of this back-scattered wave and the attenuation of the received pulse characterize the tissue interface depth (range) and the energy absorption (amplitude) data, respectively. This information may be represented in the form of an amplitude-modulated time base (A-scope, Figure 23bi). However, the information may be displayed equally well on a brightness-modulated time base in such a way that the brightness is proportional to the echo amplitude. This type of display is called a B-scan and is shown in Figure 23bii.

The B-scan illustrated in Figure 23bii corresponds to the pulse-echo information obtained along a typical scan line. It is a simple matter in principle to link the direction of the time base across the display to the direction

Figure 23.--A-scope and B-scope Displays of Ultrasonic Pulse-Echo Information.

a. Schematic representation of a section through a patient.

bi. A-scope presentation of a typical scan line.

bii. B-scope representation of the same scan line.

c. B-scan with the direction of the timebase linked to the direction of the ultrasonic beam.

d. Compound B-scan.

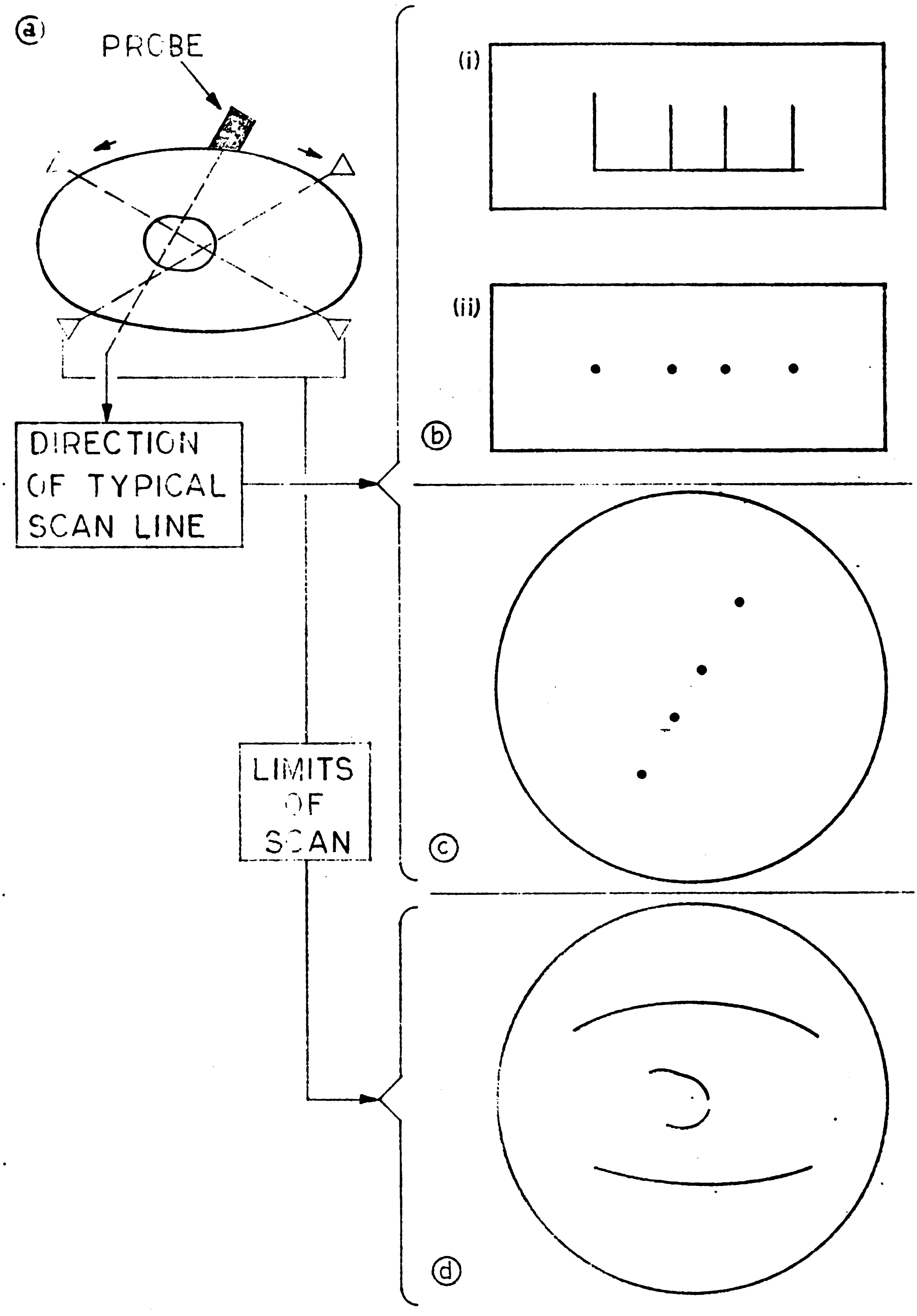

a
PROBE
(i)
(ii)
b
DIRECTION
OF TYPICAL
SCAN LINE
c
LIMITS
OF
SCAN
d

Figure 23.

of the ultrasonic beam across the patient as shown in Figure 23c. This B-scan then represents the space-position of each echo-producing interface.

If the probe is moved around the patient and all of the separate B-scans are stored on a calibrated display device or photographic plate, a picture such as shown in Figure 23d is produced. This is a "compound B-scan" and it represents a two-dimensional section through the patient in the plane of the scan.

5.3.3 Calculation of the Angle of Attack

The procedure for calculating θ the angle of attack for Doppler blood flow sensing is as follows. Several lines are drawn on the patient's skin over the vessel of interest as shown in Figure 24a. Lateral compound B-scans are performed along these lines. Each compound scan produces a two-dimensional picture as shown in Figure 24b. From the calibrated pictures, the vessel of interest is known to lie $x_1$mm from the left edge of the first scan, $x_2$mm from the left edge of the second scan, and $x_3$mm from the leftmost edge of the third compound scan. These three points are marked on the patient's skin (Figure 25a).

On the skin of the patient, a straight line is now drawn between the lateral lines 1, 2, and 3 passing through the points x_1, x_2, and x_3 (Figure 25a). A longitudinal

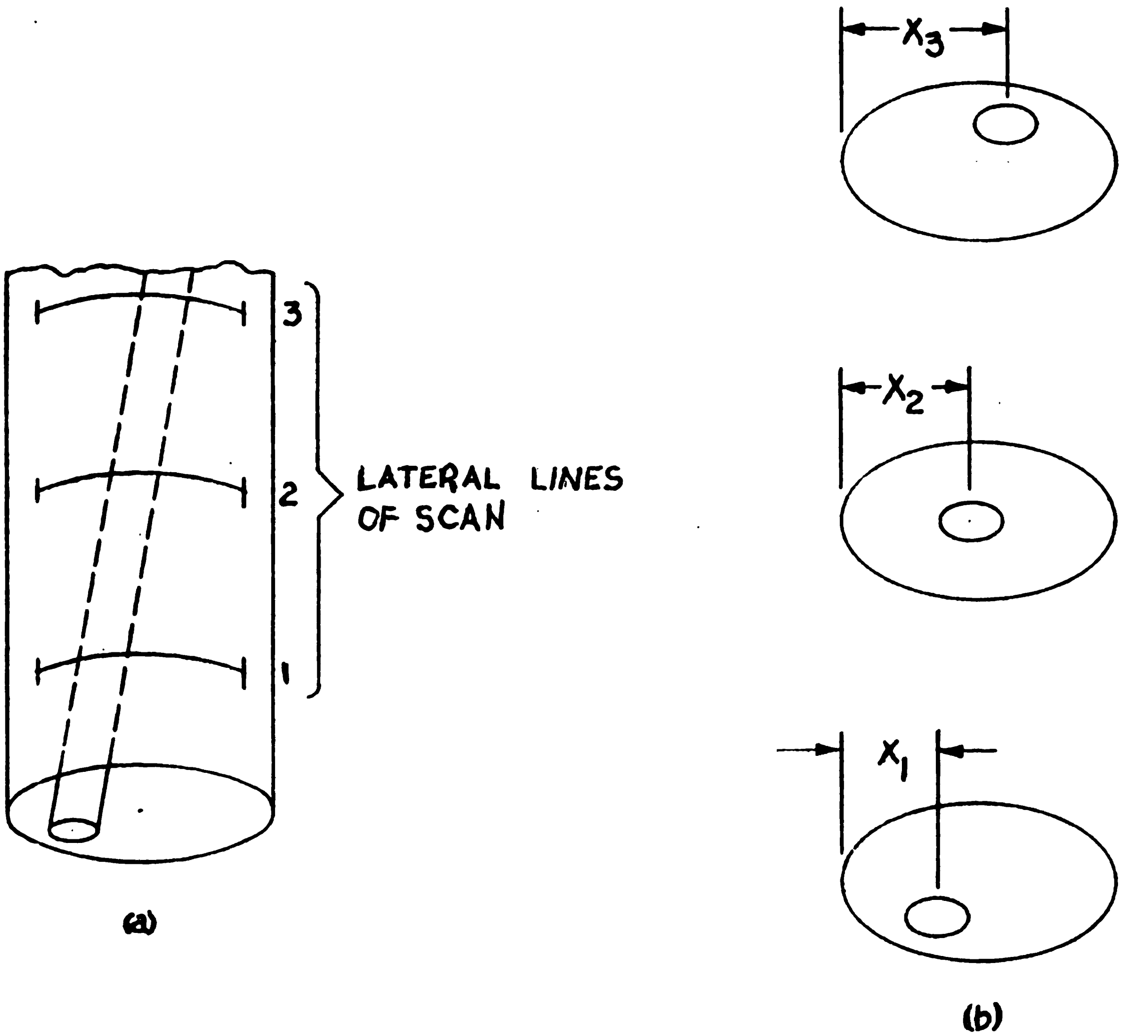

Figure 24.--Several Lateral Compound B-scans.

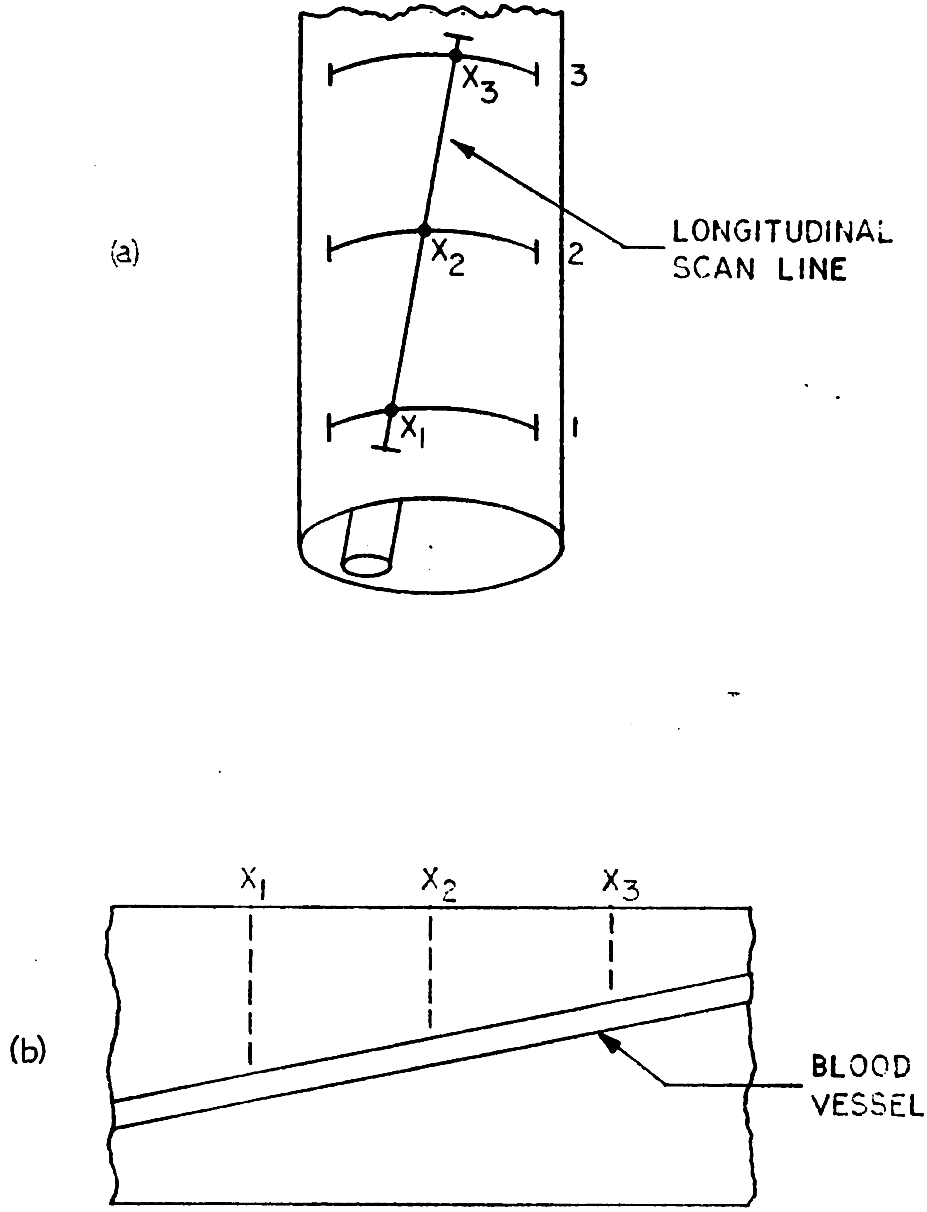

Figure 25.--Longitudinal Compound B-scan.

compound scan is performed along this constructed line. The blood vessel should be displayed from this scan as depicted in Figure 25b.

The angle α of the blood vessel relative to the surface of the skin can be computed from the photographic display depicted in Figure 25b as follows:

1. A straight line is drawn through the photographic blood vessel image.

2. The slope s of this line relative to the surface of the skin at the point x_2 is

$$s = \frac{dy}{dx} \tag{22}$$

where dy is the vertical displacement of the blood vessel, and dx is the horizontal increment.

3. α is then given by

$$\alpha = \tan^{-1} s \tag{23}$$

Figure 26 summarizes the above procedure.

With this preliminary calculation completed, ultrasonic blood flow detection may begin. The transducer positioned by its theodolite holder is acoustically coupled to the skin at the point x_2 (Figure 27). The angle β of beam incidence relative to the skin surface is read directly from the theodolite holder. With the aid of Figure 27, θ can be easily computed.

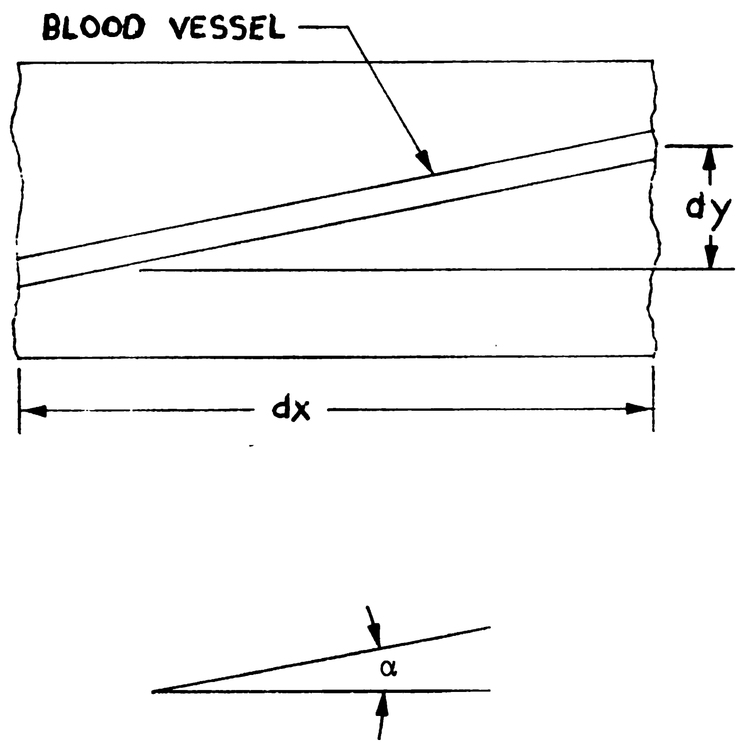

Figure 26.--Determining the Angle α.

$$\gamma = 180^{\circ} - \alpha - \beta \tag{24}$$

$$\theta = 180^{\circ} - \gamma \tag{25}$$

$$= \alpha + \beta$$

As a final check, the transducer operating in the pulsed mode should be moved such that $\theta = \alpha + \beta = 90^{\circ}$. The Doppler frequency shift should be equal to zero.

5.3.4 Conclusions

This technique determines the location of the blood vessel and computes θ the angle of ultrasonic attack. It appears to be a theoretically sound approach to the problem if the observer is experienced with the interpretation of compound B-scans. To the author's knowledge, no such method of angular calculation has been presented in the literature to date.

The main disadvantage associated with this technique is that compound B-scan storage devices are very expensive. The final accuracy of the angle measurement will have to determine if such an investment is worthwhile.

CHAPTER VI

SUMMARY

6.1 Results and Conclusions

The analysis presented in Chapter II shows that the range resolution of the random signal ultrasonic system is determined by the bandwidth of the transmitted signal. The velocity resolution is determined by the bandwidth of the filter following correlation. These bandwidths are independently controllable, thereby making it possible to make very accurate range and velocity measurements simultaneously.

The primary advantage of the random signal system is its freedom from range ambiguities. This permits the use of high pulse repetition rates to measure any given Doppler shift unambiguously in the absence of clutter. Spectrum folding, which would occur for a conventional ultrasonic system used to detect high velocity targets, is completely avoided.

In comparison to conventional pulse systems, the duty factor of the transmitted random waveform can be kept large thereby providing a greater average power for a given peak power. Increased sampling rates, duty factors and coherent or noncoherent integration all provide an improvement in the system's signal-to-noise ratio.

In Chapter III the experimental random signal ultrasonic system is described and the Doppler resolution results are presented. These results indicate that the experimental system is capable of measuring the Doppler difference frequency within an error range of $\pm$ 1%. This system does not by any means represent the ultimate capabilities of random signal ultrasonic techniques. It was built to demonstrate and verify the theoretical results. The basic system configuration and performance will continue to be improved in many ways since the initial construction.

Previous experimental work by Newhouse _et al_. [64] established the range resolution capabilities of the random signal ultrasonic system.

The theory and operation of a dual element broadband transducer [67] designed for ultrasonic blood flow detection is presented in Chapter IV. The novel transducer is compared with a single element transducer in terms of lateral range resolution. The experimental results presented in that chapter indicate a marked increase in lateral resolution with the dual element transducer.

In Chapter V, two methods for determining the angles associated with Doppler blood flow measurement are described. The first technique appears to be the accepted method for calculating these angles. The second method, developed by the author, makes use of the information obtained from several compound B-scans to determine the slope of the blood vessel and the angle of attack. Experience is required in interpreting the compound B-scans. Although the latter method is shown to be theoretically feasible, no experimental results are presented on this topic.

6.2 Recommendations for Further Work

To fully demonstrate the superiority of the random signal ultrasonic system in comparison to conventional pulse Doppler techniques, experimental results indicating the random signal-to-noise ratio are required.

Further experiments involving the use of smaller polystyrene particles (7-10 microns) or human blood should be conducted to determine the capability of the random signal system in detecting Doppler shifts from smaller sound scatterers.

It is hoped that by combining the unique lateral resolution property of the dual element transducer with the longitudinal resolution capability provided by random signal processing that velocity profiles can be obtained for deep-lying and small blood vessels.

The experimental feasibility of employing the compound B-scan technique to the transcutaneous calculation of the ultrasonic angles of attack needs to be demonstrated.

Finally some theoretical work must be undertaken to determine if the equation used to relate the velocity of the moving target to the Doppler shift frequency (equations 2 and 19) is still valid for bandlimited random processes. The derivation of this formula assumes that only a single frequency f_o is transmitted. In the random signal ultrasonic system, f_o is interpretted as the center frequency of the bandlimited random signal generated.

REFERENCES

REFERENCES

1. Franklin, D. L., Schegel, W. A. and Watson, N. W., "Ultrasonic doppler shift blood flowmeter," Biomed. Seis, Instrum. I, p. 309-315, 1963.

2. Kaneko, Z., Shirashi, J., Omizo, H., Kato, K., Motomiya, M., Izumi, T. and Okumura, T., "Analyzing blood flow with sonograph," Ultrasonic 4, p. 22-23, 1966.

3. Strandness, D. E., McCutcheson, E. P., and Rushmer, R. F., "Application of a transcutaneous doppler flowmeter in evaluation of occlusive arterial disease," Surg. Gynec. Obstet., 122, p. 1039-1045, 1966.

4. Strandness, D. E., Schultz, R. D., Summer, D. S., and Rushmer, R. F., "Ultrasonic flow detection. A useful technique in the evaluation of peripherial vascular disease," Am. J. Surg., 113, p. 311-320, 1967.

5. Baker, D. W., "Pulsed doppler blood-flow sensing," IEEE Transactions on Sonics and Ultrasonics, Vol. SU-17, No. 3, p. 170-185, July 1970.

6. Gould, K. L., Mozersky, D. J., Hokanson, D. E., Baker, D. W., Kennedy, J. W., Sumner, D. S., and Strandness, D. E., Jr., "A noninvasive technic for determining patency of saphenous vein coronary bypass grafts," Circulation, Volume XLVI, p. 595-600, September 1972.

7. Yoshida, T., Mori, M., Minura, Y., Kikita, G., Takagish, S., Nakanishi, K., and Satomura, S., "Analysis of heart motion with ultrasound doppler method and its clinical application," American Heart Journal 61, p. 61-75, 1961.

8. Yoshitoshi, Y., Machii, K., Seldiguchi, H., Mishina, Y., Ohta, S., Hanaoka, Y., Shimizu, S., and Kuno, H., "Doppler measurement of mitral valve and ventrical wall velocities," Ultrasonics 4, p. 27-28, 1966.

9. Feigenbaum, H., "Diagnostic ultrasound as an aid to the management of patients with paricardial effusion," Chest, p. 55-59, 1969.

10. McDonald, I. G., Feigenbaum, H., and Chang, Sonia, "Analysis of left ventricular wale motion by reflected ultrasound. Application to assessment of myocardial function," Circulation, Volume XLVI, p. 14-25, July 1972.

11. Sweatman, T., Selzer, A., Kamagaki, M., and Cohn, K., "Echocardiographic diagnosis of mitral regurgitation due to ruptured chordae tendineae," Circulation, Volume XLVI, p. 580-586, September 1972.

12. Meyer, R. A. and Kaplan, S. K., "Echocardiography in the diagnosis of hypoplasia of the left or right ventricles in the neonate," Circulation, Volume XLVI, p. 55-64, July 1972.

13. Lundstrom, N. R., "Echocardiography in the diagnosis of congenial mitral stenosis and in evaluation of the results of mitral valvotomy," Circulation, Volume XLVI, p. 44-54, July 1972.

14. Tajik, A. J., Gau, G. T., Ritter, D. G. and Schattenberg, T. T., "Echocardiographic pattern of right ventricular diastolic volume overload in children," Circulation, Volume XLVI, p. 36-43, July 1972.

15. Fortum, N. J., Hood, W. P., Jr., and Craige, E., "Evaluation of left ventricular function by echocardiography," Circulation, Volume XLVI, p. 26-35, July 1972.

16. Freeman, J. J., Hitt, J. S., Rinalds, J. A., "A system for the detection of mitral valvular disease," Proc. IEEE Kelly communication conference, 1970.

17. Fry, F. J., Heimburger, R. F., Gibbons, L. V., and Eggleton, R. C., "Ultrasound for visualization and modification of brain tissue," IEEE Transaction on Sonic and Ultrasonics, Vol. SU-17, No. 3, p. 165-170, July 1970.

18. Callagan, D. A., Rowland, T. C., and Goldman, D. E., "Ultrasonic doppler observation of the fetal heart," Obst. Gync., N. Y. 23, 637, 1964.

19. Fielder, F. D. and Pocok, P., "Foetal Blood detector," Ultrasonics, 6, p. 240-241, 1968.

20. Johnson, W. L., Stegall, H. F., Leim, J. N. and Rushmer, R. F., "Detection of fetal life in early pregnancy with ultrasonic doppler flowmeter," Obst. Gyn. N. Y. 26, p. 305-307, 1965.

21. Rushmer, R. F., Baker, D. W., and Stegall, H. F., "Transcutaneous doppler flow detection as nondestructive technique," J. Appl. Physiol. 21, p. 554-566, 1966.

22. Wells, P. N. T., "Physical principles of ultrasonic diagnosis," Academic Press, London, 1969.

23. Lathi, B. P., "Communication systems," John Wiley and Sons, Inc., 1968.

24. Dintentass, Leopold, "Blood rheology in ischemic diseases," Proceedings of the 8th International Conference on Medical and Biological Engineering, Session 1-1, July 1969.

25. Baker, D. W. and Strandness, D. E., "Instrumentation for early detection of arterial occlusive disease," Proceedings of the 8th International Conference on Medical and Biological Engineering, Session 1-8, July 1969.

26. Cohen, M. V., Cohn, P. F., Herman, M. V., and Gorlin, R. G., "Diagnosis and prognosis of main left coronary artery obstruction," Supplement I to Circulation, Vols. XLV and XLVI, p. I-57-I-65, May 1972.

27. Dunn, F. and Fry, F. J., "Ultrasonic threshold dosage for the mammalian central nervous system," IEE Transaction on Biomedical Engineering, Vol. BME-18, No. 4, p. 253-256, July 1967.

28. Ulrich, W. D., "Ultrasound dosage for experimental use on human beings," Naval Medical Research Inst., Bethesda, Md., AD-731 075, 15p., August 19, 1971.

29. Hamilton, Andrew, "Seeing your ailments with sound," Today's Health, Vol. 46, p. 20-24, March 1968.

30. Franklin, D. L., "Techniques for measurement of blood flow through intact vessels," Med. Electron. Biol. Engng., Vol. 3, p. 27-37, Pregman Press, 1965. Printed in Great Britain.

31. Kalmus, H. P., "Electronic flowmeter system," Rev. Scient. Instrum., 25, p. 201-206, 1954.

32. Haugen, M. G., Farral, W. R., Herrick, J. F., and Baldes, G. J., "An ultrasonic flowmeter," Proc. Nat. Electron. Conf., II, p. 465-475, 1955.

33. Baldes, G. J., Farrall, W. R., Haugen, M. C., and Herrie, J. F., "A forum on an ultrasonic method for measuring the velocity of blood," p. 165-176, Ultrasound in Biology and Medicine (ed. E. Kelly) A.I.B.S., Washington, 1957.

34. Franklin, D. L., Baker, D. W., Ellis, E. M., and Rushmer, R. F., "A pulsed ultrasonic flowmeter," I.R.E. Trans, Med. Electron. Me-6, p. 204-2-6, 1959.

35. Franklin, D. L., Baker, D. W., and Rushmer, R. F., "Pulsed ultrasonic transit time flowmeter," Ins. Rad. Engrs. Trans. Bio-Med. Electron, BME-9, p. 44-49.

36. Farrall, W. R., "Design considerations for ultrasonic flowmeters," I.R.E. Trans. Med. Electron. ME-6, p. 198-201, 1959.

37. Zarnstroff, W. D., Castillo, C. A., Crumpton, C. W., "A phase shift ultrasonic flowmeter," Inst. Rad. Engrs. Trans. Bio-Med. Electron. BME-9, p. 199, 1962.

38. Nobel, F. W., Goldsmith, T. C., Waldsburger, C. J., and Cook, T. E., "A new system for measurement of blood flow by ultrasonics," Digest of 15th Conference on Engineering in Medicine and Biology, Chicago, 1962.

39. Wetterer, E., "A critical appraisal of methods of blood flow determination in amimals and man," I.R.E. Trans. Med. Electron. Me-9, p. 165-173, 1962.

40. Arts, M. G. J., and Roevors, J. M., "On the instantaneous measurement of blood flow by ultrasonic means," Med. and Biol. Engng., Vol. 10, p. 232-34, 1972.

41. Green, P. S., "Spectral broadening of acoustic reverberation in doppler shift fluid flowmeters," J. Acoust. Soc. Am., 36, p. 1383-1390, 1964.

42. Satomura, S., "Study of the flow pattern in peripheral arteries by ultrasonics," J. Acoust. Soc., Japan, Vol. 15, 1959, p. 151-158.

43. Franklin, D. L., Schlegel, W. A., and Rushmer, R. F., "Blood flow measured by doppler frequency shift of backscattered ultrasound," Science, Vol. 132, 1961, p. 564-565.

44. Baker, D. W., et al., "A sonic transcultaneous blood flowmeter," Proc. 17th Am. Conf. on Engng. Med. Biol., 1964, p. 76.

45. McLeod, F. D., "A doppler ultrasonic physiological flowmeter," Proc. 17th Am. Conf. on Engng. Med. Biol., 1964, p. 81.

46. McLeod, F. D., "A directional doppler flowmeter," Digest of the 7th Conf. Med. Biol. Engng., Stockholm, Sweden, 1967.

47. Yoshitoshi, Y., Machii, K., Sekiguchi, H., Mishima, Y., Ohta, S., Hanaoka, Y., Kohashi, Y., Shimuzu, S., and Kuno, H., "Doppler measurement of mitral valve and ventricle wall velocities," Ultrasonics, Vol. 4, 1966, p. 27-28.

48. Watson, B. W. (Editor), "IEE medical electronics monographs," Peter Peregrinus Ltd., 1971.

49. Barnes, R. W. and Thurstone, F. L., "An ultrasound moving target indicator system for diagnostic use," IEEE Trans. on Bio-Med. Eng., Vol. 18, January 1971, p. 428.

50. Flaherty, J. J. and Strauts, E. J., "Ultrasonic pulse doppler instrumentation," 8th International Conference on Medical and Biological Engineering, Chicago, 1969.

51. Peronneau, P. A. and Leger, F., "Doppler ultrasonic pulsed blood flowmeter," 8th International Conference on Medical and Biological Engineering, Chicago, 1969.

52. Hokanson, D. E., Mozersky, D. J., Summer, D. S., and Strandness, D. E., "Ultrasonic arteriography and phase-locked echo tracking system for measuring arterial diameter changes," IEEE Ultrasonic Symposium, Miami Beach, 1971.

53. McLeod, F. D. and Anliver, M., "Multiple gate pulse doppler flowmeter," IEEE Ultrasonic Symposium, Miami Beach, 1971.

54. Peronneau, P., Pellet, M., Burgon, J., Xhaard, J., Hinglasis, N., Latil, F., and Couillard, F., "An ultrasonic multigated pulsed Doppler velocimeter for real time measurement of blood velocity profiles," 25th Annual Conference on Engineering in Medicine and Biology, pp. 180, 1972.

55. Skolnik, M. E., "Introduction to radar systems," McGraw-Hill, 1962.

56. Wagg, R. C., and Gramiak, R., "Noninvasive heart blood flow rate measurement," Presented at 16th Annual Meeting of the American Institute of Ultrasound in Medicine, Denver, Colorado, 19-22 October 1971.

57. Wagg, R. C., Rhoads, W. L., and Gramiak, R., "Instrumentation for noninvasive cardiac chamber flow rate measurement," IEEE Ultrasonic Symposium Boston October 4-7, 1972.

58. McGillem, C. D., Cooper, G. R., Waltman, W. B., "Use of wideband stochastic signals for measuring range and velocity," EASCON Conference Record, pp. 305-311, 1969.

59. Cooper, G. R. and R. L. Gassner, "Analysis of a wide band random signal radar system," Purdue University, TR-EE 66-9, August, 1966.

60. Cooper, G. R. and C. D. McGillem, "Random signal radar," Purdue University, TR-EE-67-11, June, 1967.

61. Cooper, G. R. and R. J. Purdy, "Detection, Resolution, and accuracy in the random signal radard," Purdue University, TR-EE-68-16, August, 1968.

62. C. D. McGillem and W. B. Waltman, "An experimental random signal radar system," Purdue University, TR-EE-69-46, December, 1969.

63. Rihaczek, Principle of High-Resolution Radar, McGraw Hill, 1969.

64. Newhouse, V., Cooper, G., Feigenbaum, H., Jethwa, C. P., and Kaveh, M., "Ultrasonic blood velocity measurement using random signal correlation techniques." Invited for a presentation at the 10th International Conference on Medical and Biological Engineering, Dresden, GDR, August 13-17, 1973.

65. Egli, P. H., "Ultrasonic beam transducer," United States Patent Number 786,258, December 1968.

66. Wilkox, M. H., and Egli, P. H., "Ultrasonic-Amplitude-Dopper Detector," United States Patent Number 787, 397, December 1968.

67. Jethwa, C. P., Saggio, Frank III, "Resolution of a pulsed random signal ultrasonic doppler system." Accepted for a presentation at the 18th annaul meeting of the American Institute of Ultrasound in Medicine, Ann Arbor, Michigan, October 14-18, 1973.

68. Chadwick, Russell B., "Use of random signals to study distributed radar targets," Ph.D. thesis, School of Electrical Engineering, Purdue University, August 1970.

69. L. A. Geddes, "Measurement of blood pressure," Year Book Medical Publishing, Inc. 1970.

70. McCutchen, E. P. and Rushmer, R. F., "Korotkoff Sounds," Circulation Res. 20:149-161, 1967.

71. Tursky, B., Shapiro, D., Schwartz, G. E., "Automated constant cuff-ressure system to measure average systolic and diastolic blood pressure in man," IEEE Transaction on Biomedical Engineering, Volume RME-19, Number 4, pp. 271-276.

72. Sigel, B., Gibson, R., Amatneek, K., Felix, R., Edelstein, A., Popky, G., "A Doppler ultrasound method for distinguishing laminar from turbulent flow," Journal of Surgical Research, Vol. 10, No. 5, pp. 221-224, May 1970.

73. Satomura, S., "Ultrasonic Doppler method for the inspection of cardiac functions." J. Acoust. Soc. Am., 29, pp. 1181-1185, 1957.

74. Lube, V. M., Safonov, Yu. D. and Yakiemenkov, L. I., "Ultrasonic detection of motions of cardiac valves and muscle." Soviet Phys. Acoust. 13, pp. 59-65, 1967.

MICHIGAN STATE UNIV. LIBRARIES
31293003838731